Title

MafF is an antiviral host factor that suppresses transcription from Hepatitis B Virus core promoter

Running title

MafF restricts HBV replication

Authors

Marwa K. Ibrahim[1,2], Tawfeek H. Abdelhafez[1,2], Junko S. Takeuchi[1,3,4], Kosho Wakae[1], Masaya Sugiyama[5], Masataka Tsuge[6], Masahiko Ito[7], Koichi Watashi[1], Mohamed El Kassas[8], Takanobu Kato[1], Asako Murayama[1], Tetsuro Suzuki[7], Kazuaki Chayama[6], Kunitada Shimotohno[9], Masamichi Muramatsu[1#], Hussein H. Aly[1#], Takaji Wakita[1]

Affiliation

[1]Department of Virology II, National Institute of Infectious Diseases, 1-23-1 Toyama, Shinjuku-ku, Tokyo 162-8640, Japan
[2]Department of Microbial Biotechnology, Division of Genetic Engineering and Biotechnology Research, National Research Centre, 33 EL Bohouth St. (formerly El Tahrir St.), Dokki, Giza, P. O. 12622, Egypt
[3]Center for Clinical Sciences, National Center for Global Health and Medicine, Tokyo, Japan
[4]Organization for the Strategic Coordination of Research and Intellectual Properties, Meiji University, Kanagawa, Japan
[5]Genome Medical Sciences Project, National Center for Global Health and Medicine, 1-7-1 Kohnodai, Ichikawa, Chiba, 272-8516, Japan
[6]Department of Gastroenterology and Metabolism, Graduate School of Biomedical and Health Science, Hiroshima University, 1-2-3 Kasumi, Minami-ku, Hiroshima, 734-8551, Japan
[7]Department of Virology and Parasitology, Hamamatsu University School of Medicine, 1-20-1 Handayama, Higashi-ku, Hamamatsu, Shizuoka, 431-3192, Japan
[8]Endemic Medicine Department, Faculty of Medicine, Helwan University, Cairo, P. O. 11795, Egypt
[9]Center for Hepatitis and Immunology, National Center for Global Health and Medicine, Chiba 272-8516, Japan

Corresponding Authors

Hussein H. Aly, email: ahussein@nih.go.jp

Masamichi Muramatsu, email: muramatsu@nih.go.jp

The word count for the abstract: 247 words

The word count for the text: 6059 words

Abstract

Hepatitis B Virus (HBV) is a stealth virus that exhibits only minimal induction of the interferon system that is required for both innate and adaptive immune responses. However, 90% of acutely infected adults can clear the virus, suggesting the presence of additional mechanisms that facilitate viral clearance. Herein, we report that Maf bZIP transcription factor F (MafF) promotes host defense against infection with HBV. Using siRNA library and an HBV/NL reporter virus, we screened to identify anti-HBV host factors. Our data showed that silencing of *MafF* led to a 6-fold increase in luciferase activity after HBV/NL infection. Overexpression of MafF reduced HBV core promoter transcriptional activity, which was relieved upon mutating the putative MafF binding region. Loss of MafF expression by CRISPR/CAS9 (in HepG2-hNTCP-C4 cells) or siRNA silencing (in primary hepatocytes [PXB]), induced HBV core and HBV pregenomic RNA (pgRNA) levels, respectively, after HBV infection. MafF physically binds to HBV core promoter and competitively inhibits HNF-4α binding to an overlapping sequence in HBV enhancer II sequence (EnhII) as seen by ChIP analysis. MafF expression was induced by IL-1β/TNF-α treatment in both HepG2 and PXB cells, in an NF-κB-dependent manner. Consistently, *MafF* expression levels were significantly enhanced and positively correlated with the levels of these cytokines in patients with chronic HBV infection, especially in the immune clearance phase.

62 **Importance**

63 HBV is a leading cause of chronic liver diseases, infecting about 250 million people
64 worldwide. HBV has developed strategies to escape interferon-dependent innate immune
65 responses. Hence, the identification of other anti-HBV mechanisms is important for
66 understanding HBV pathogenesis, and developing anti-HBV strategies. MafF was shown to
67 suppress transcription from HBV core promoter, leading to a significant suppression of HBV
68 life cycle. Furthermore, MafF expression was induced in chronic HBV patients and in
69 primary human hepatocytes (PXB). This induction correlated with the levels of inflammatory
70 cytokines (IL-1β and TNF-α). These data suggest that the induction of MafF contributes to
71 the host's antiviral defense by suppressing transcription from selected viral promoters. Our
72 data shed light on a novel role for MafF as anti-HBV host restriction factor.

73
74
75
76
77
78
79
80
81
82
83
84
85
86
87
88
89

Introduction

In the earliest stages of viral infection, the host initially detects and counteracts infection via induction of innate immune responses (44). Host restriction factors are essential components of the innate antiviral immune response; these factors serve critical roles in limiting virus replication before the adaptive immune response engages to promote virus clearance (5). These antiviral restriction factors are typically induced by cytokines, including interferons (IFNs) (52), transforming growth factor-beta (TGF-β) (28), and interleukin-1-beta (IL-1β) (54). These restriction factors suppress viral replication by targeting the infection at various stages of the virus life cycle, including viral entry (3), transcription of the viral genome (63), viral RNA stability (2), translation of viral proteins (32), viral DNA replication (33), and production of viral particles (6).

Approximately 250 million people worldwide are chronically infected with Hepatitis B virus (HBV). These patients are at high risk of developing life-threatening complications, including hepatic cirrhosis, hepatic failure, and hepatocellular carcinoma. Current treatments include nucleos(t)ide analogs that efficiently suppress HBV replication. However, an HBV replication intermediate, covalently closed circular DNA (cccDNA), persists in the nucleus. The cccDNA intermediate gives rise to progeny virus, and may lead to the development of drug-resistant mutants and/or relapsing HBV after drug withdrawal (41). As such, new strategies for HBV treatment are needed.

HBV has been identified in human remains from ~7000 years ago (26). This prolonged history and evolution has shaped HBV to be one of the most successful of the "stealth" viruses that can successfully establish infection while evading IFN induction (62). Although HBV can evade IFN induction, the majority of HBV-infected adults (90%) are ultimately able to clear the virus. This observation suggests that there are likely to be one or more IFN-independent host restriction factors that facilitate HBV clearance.

The small Maf proteins (sMafs) are a family of basic-region leucine zipper (bZIP)-type transcription factors. MafF, MafG and MafK are the three sMafs identified in vertebrate species (23). sMafs lack a transcriptional activation domain hence, they can act as both transcription activator or repressor based on their expression levels and dimerization partners

119 (18). Intriguingly, previous reports have documented induction of MafF in myometrial cells
120 by inflammatory cytokines, including IL-1β and tumor necrosis factor alpha (TNF-α) (31).
121 However, there have been no previous studies that have addressed a role for MafF in
122 promoting an antiviral innate immune response.

123 Using an HBV reporter virus and an siRNA library, we performed functional siRNA
124 screening to identify the host factors that influence the HBV life cycle. Based on the results
125 of this screen, we identified MafF as a negative regulator of HBV infection. Further analysis
126 revealed that MafF functions as a repressor of transcription at the HBV core promoter,
127 thereby suppressing HBV replication. This is the first study to report a role for MafF as an
128 anti-HBV host factor that represses transcription from the promoters of susceptible viruses.
129
130
131
132
133
134
135
136
137
138
139
140
141
142
143
144
145
146
147

148 **Results**

149

150 **1. MafF suppresses expression of the HBV/NanoLuc (NL) reporter virus**

151 HBV particles carrying a chimeric HBV virus encoding NanoLuc (NL) were prepared as
152 previously described (43). Since these particles carry a chimeric HBV genome in which HBc
153 is replaced by NL, the NL levels released after infection with these particles can only detect
154 the early stages of HBV infection from entry to transcription of HBV-pgRNA (43). We used
155 this high-throughput system, in combination with druggable genome siRNA Library, to
156 screen for host factors that influence these early stages. This approach facilitated testing of
157 2200 human genes for their influence on the HBV life cycle. Screening was performed in
158 HepG2-C4 cells that express the HBV entry receptor, hNTCP (17). Non-targeting siRNAs,
159 and siRNAs against h*NTCP*, were used as controls for each plate (Fig. 1A). Cellular viability
160 was determined using the XTT assay; wells with ≥20% loss of cell viability were excluded
161 from further evaluation. NL activity was induced more than 5 folds (average of 3 different
162 siRNAs) upon the independent silencing of only 10 out of the 2200 host genes (0.4%). These
163 genes were identified as anti-HBV host factors, and based on the induction level of NL
164 activity, these genes were classified into 3 groups: Genes in which NL activity ranged from
165 5 to 10 folds (n=6 genes, MafF fits in this group), from 10 to 20 folds (3 genes), and from 20
166 to 30 folds induction of NL activity (1 gene) (Fig. 1A). MafF was one the anti-HBV host
167 factors identified by this screening. MafF was previously reported to be induced by famous
168 inflammatory cytokines (IL-1b, and TNF-a), one of the common criteria of anti-viral host
169 restriction factors (28, 52, 54), hence we decided to analyze its role on HBV life cycle.
170 Silencing of *MafF* expression with si-1 or si-3 resulted in 6- ($p < 0.0001$) or 10-fold ($p <$
171 0.001) increases in NL activity, respectively, compared to that observed in cells transfected
172 with the control siRNA (Fig. 1B). The MafF-specific sequence, si-2, did not show a similar
173 effect on NL activity (Fig. 1B). This result was consistent with the fact that si-2 had a lower
174 silencing efficiency for MafF (Fig. 1C). Since NL activity was measured 10 days after
175 siRNA silencing of *MafF* expression, we measured the MafF protein levels at the designated

176 time in order to confirm the prolonged silencing of *MafF* by si-3 (Fig. 1D). Taken together,
177 these findings suggest that MafF may suppress HBV infection.
178
179
180 **2. MafF strongly suppresses HBV core promoter activity**
181 The HBV/NL reporter system can be used to detect factors affecting the early steps of the
182 HBV life cycle, from HBV entry through cccDNA formation, transcription and translation
183 of HBV-pgRNA (43). Silencing of *MafF* had no impact on cccDNA levels observed in cells
184 infected with HBV as shown by real-time PCR (Fig. 2A) and by southern blot (Fig. 2B);
185 these results indicated that MafF suppressed the HBV life cycle at stage that was later than
186 that of cccDNA formation. Given that MafF can induce transcriptional suppression (18), we
187 analyzed the impact of MafF on various HBV promoters (core, X, preS1, and preS2) using a
188 reporter system in which firefly luciferase coding sequence was inserted downstream to the
189 corresponding HBV promoter. We found that overexpression of MafF resulted in significant
190 suppression of transcription from the HBV core promoter (approximately 8-fold; $p<0.0001$),
191 and significant, albeit less of an impact on transcription from the HBV-X and preS1
192 promoters (both at approximately 2-fold, $p<0.0001$); overexpression of MafF had no
193 significant impact on transcription from the preS2 promoter (Fig. 2C left panel). Likewise,
194 siRNA silencing of endogenous *MafF* enhanced HBV core promoter activity (Fig. 2C right
195 panel, $p<0.0001$). Since the NanoLuc gene in HBV/NL virus (Fig. 1B) is transcribed from
196 an HBV core promoter (43), the findings presented in Fig. 1 and Fig. 2 collectively suggest
197 that MafF-mediated suppression of HBV is mediated primarily by inhibition of transcription
198 from the core promoter.
199
200 **3. MafF suppresses HBV replication**
201 The HBV core promoter controls the transcription of the longest two HBV RNA transcripts,
202 the precore and pgRNAs. HBeAg is translated from the HBV precore RNA, while translation
203 of HBV-pgRNA generates both the polymerase (Pol) and the capsid subunit; the pgRNA also
204 serves as the template for HBV-DNA reverse transcription (4, 14). As such, we assumed that

205 MafF served to inhibit HBV replication by controlling transcription of the HBV core
206 promoter. In fact, overexpression of MafF resulted in significant suppression of the pgRNA
207 titer of HBV genotypes A and D, as demonstrated by RT-qPCR (Fig. 3A, $p<0.0001$ for each
208 genotype). Overexpression of MafF also suppressed the release of HBeAg as measured by
209 enzyme-linked immunosorbent assay (ELISA) (Fig. 3B, $p<0.0001$), as well as the
210 intracellular accumulation of HBV core protein as detected by immunoblotting (Fig. 3C
211 upper and lower panels; $p<0.05$ by densitometric analysis) and the level of HBV core-
212 associated DNA as revealed by southern blot (Fig. 3D).
213
214 **4. MafF-KO induce HBV core protein levels**
215 To further clarify the significance of MafF on HBV infection, we established CRISP/CAS9
216 MafF-KO HepG2-hNTCP-C4 cells. Out of 11 selected clones, MafF-KO-8 and 11 showed
217 the best KO phenotype (Fig. 4A). Myrcludex-B is a lipopeptide consisting of amino acid
218 residues 2–48 of the pre-S1 region of HBV, and is known to block HBV entry [18], pre-
219 treatment with Myrcludex-B (1 μM) 1 hour before infection was performed to confirm that
220 the detected signals were derived from HBV infection and did not represent non-specific
221 background(12). Both MafF-KO-8 and 11 showed a higher NL secretion after HBV/NL
222 infection when compared to parental HepG2-hNTCP-C4 cells with values ranging from 1.5
223 to 3 folds respectively (Fig. 4B). Accordingly, MafF-KO-11 showed 4 times higher HBc
224 levels after HBV infection (Fig. 4C right and left panels). In comparison to the original
225 HepG2-hNTCP-C4 cells, MafF-KO-11 cells showed similar levels of secreted HBs after
226 HBV infection (Fig. 4D), which can be explained by the major function of MafF as a
227 transcriptional repressor of HBV core promoter with minimal to no effect of PreS1 and PreS2
228 promoters (Fig. 2 B and C).
229
230 **5. MafF binds to the HBV core promoter**
231 MafF is a member of (Maf) family of transcription factors, bZIP-type transcription factors
232 that bind to DNA at Maf recognition elements (MAREs). MAREs were initially defined as a
233 13-bp (TGCTGA(G/C)TCAGCA) or 14-bp (TGCTGA(GC/CG)TCAGCA) elements (21,

234 24). The specificity of this binding sequence is greatly affected by the dimerization partners
235 of MafF; multiple studies have presented findings suggesting heterogeneity within MARE
236 sequences, especially when MafF heterodimerizes with another bZIP-type transcription
237 factors (25, 42, 49). We next analyzed the HBV core promoter for putative MafF binding
238 region using the JASPAR database of transcription factor binding sites (51). Toward this end,
239 we identified the sequence 5'-TGGACTCTCAGCG-3' that corresponded to nucleotides (nts)
240 1667 to 1679 of the HBV-C_JPNAT genome (GenBank AB246345.1) in the enhancer 2
241 (EnhII) of the HBV core promoter. This motif shared a similarity to a previously defined Maf
242 responsive element (MARE) (18) and also with the DNA binding site for other cap'n'collar
243 (CNC) family proteins Nrf1, Nrf2, Bach1 (Jaspar matrix profiles, MA0506.1, MA0150.1,
244 and MA0591.1, respectively), and bZIP transcription factors that are reported to
245 heterodimerize with sMafs (Fig. 5A). As such, we evaluated the role of this predicted
246 MafF/bZip site with respect to HBV core promoter activity. We found that the 9th and 11th
247 nucleotides of the aforementioned predicted MafF binding region, which are A and C,
248 respectively, are highly conserved common residues in the predicted MafF/bZip binding
249 sequence (Fig. 5A). We disrupted this predicted MafF/bZip site by introducing 2-point
250 mutations (A1676C and C1678A) into the HBV core promoter (Fig. 5A). Despite a minimal
251 but statistically significant reduction of HBV core promoter activity induced by the
252 introduction of these mutations (Fig. 5B right panel, $p<0.0001$), MafF overexpression
253 suppressed the wild-type (WT) core promoter 2–3 times more than that carrying mutations
254 (A1676C and C1678A) (Fig. 5B left panel, $p<0.0001$). Furthermore, ChIP analysis revealed
255 that there was significantly less physical interaction between MafF and the HBV core
256 promoter with A1676C and C1678A mutations than was observed between MafF and the
257 HBV WT counterparts (Fig. 5C, $p<0.05$ for % of input and $p<0.01$ for fold enrichment).
258 These results confirmed that MafF physically binds to the WT HBV core promoter at the
259 putative MafF/bZIP binding region and thereby suppresses transcription. Interestingly the 5'
260 end of the identified MafF/bZip binding region in HBV core promoter showed high
261 conservation in all HBV genotypes, while 3' end showed a relatively less conservation in
262 HBV genotypes A to E, with more sequence divergence in new world HBV genotypes F, G

263 and H (Fig. 5D). The role of these mutations in the escape from MafF-mediated
264 transcriptional repression in these genotypes needs to be further analyzed.

265 **6. MafF is a competitive inhibitor of hepatocyte nuclear factor (HNF)-4α binding to**
266 **HBV EnhII**

267 HNF-4α is a transcription factor that has been previously reported to bind HBV core
268 promoter and to induce its transcriptional activity (30, 48, 65). We found that the predicted
269 MafF binding region in the EnhII overlaps with an HNF-4α binding site that is located
270 between nucleotides 1662 to 1674 of the HBV C_JPNAT core promoter (10) (Fig. 6A). This
271 finding suggests the possibility that MafF may compete with HNF-4α at these binding sites
272 within the EnhII region. To examine this possibility, we constructed a deletion mutant of
273 EnhII/Cp (EnhII/CpΔHNF-4α#2) that extends from nt 1591 to nt 1750; this construct
274 includes the overlapping binding regions identified for MafF and HNF-4α (i.e., HNF-
275 4α site #1 at nt 1662–1674) but lacks the second HNF-4α binding site (HNF-4α site #2 at nt
276 1757–1769) as shown in Fig. 6A. We performed a ChIP assay and found that the interaction
277 between HNF-4α and EnhII/CpΔHNF-4α #2 was significantly reduced in the presence of
278 MafF (Fig. 6B, $p<0.01$ for % of input and $p<0.05$ for fold enrichment). Furthermore, MafF
279 had no impact on the expression of HNF-4α (Fig. 6C). Together, these data indicated that
280 MafF interacts directly with the HBV core promoter at the putative binding region and
281 suppresses the transcriptional activity of the HBV core promoter by competitive inhibition
282 of HNF-4α binding at an overlapping site in the EnhII region. This competitive suppression
283 is due to partial overlapping of HNF4-α and the putative MafF binding regions in HBV core
284 promoter and did not affect other host genes like ApoA1 and HNF1A known to be regulated
285 by HNF-4α (36, 59) (Fig. 6D).

286

287 **7. IL-1β and TNF-α-mediated induction of MafF expression *in vitro***

288 Given these findings, we speculated that MafF expression might be induced in hepatocytes
289 in response to HBV infection. Based on a previous report of the induction of MafF by both
290 IL-1β and TNF-α in myometrial cells (31), and the fact that both of these cytokines have

291 been implicated in promoting host defense against HBV, we explored the possibility that
292 MafF might be induced by one or more of these cytokines in our *in vitro* system. As shown
293 in Fig. 7, addition of IL-1β or TNF-α resulted in significant induction of *MafF* mRNA
294 expression in HepG2 cells (Fig. 7A, $p<0.0001$ for each cytokine); MafF protein was also
295 detected at higher levels in HepG2 cells exposed to each of these cytokines (Fig. 7B). NF-
296 κB is a downstream regulatory factor that is shared by the IL-1β and TNF-α signaling
297 pathways. We found that chemical inhibition of NF-κB activity with Bay11-7082 or BMS-
298 3455415 suppressed the induction of *MafF* expression in response to IL-1β (Fig. 7C, D;
299 $p<0.05$ for each of these inhibitors) and to TNF-α (Fig. 7E; $p<0.01$). These findings indicate
300 that the IL-1β and TNF-α–mediated induction of *MafF* expression in hepatocytes is regulated
301 by NF-κB signaling. Since we showed that MafF competes with HNF-4α for its interaction
302 with HBV core promoter (Fig. 6), we hypothesized that this effect can be enhanced by IL-
303 1β. We performed a ChIP assay and found that 3 hours after treatment with IL-1β, the
304 interaction between HNF-4α and EnhII/CpΔHNF-4α #2 was significantly reduced. This
305 effect was partially reversed when *MafF* expression was silenced (Fig. 7F, $p<0.01$ for % of
306 input and fold enrichment). These data mechanistically explain the role of MafF on the
307 suppression of HBV core promoter activity by the inflammatory cytokine IL-1β.
308

309 **8. MafF targets HBV infection in human primary hepatocytes**

310 Loss-of-function experiment in the primary hepatocytes is the ideal experimental platform to
311 analyze the physiological significance of endogenous MafF on the HBV life cycle. We
312 silenced *MafF* expression in human primary hepatocytes (PXB cells) using two independent
313 siRNAs, including si-3, which efficiently targets the *MafF* transcript, and si-2, which was
314 associated with a negligible silencing efficiency (Fig. 1C and Fig. 8A, upper panels) followed
315 by infection with HBV (genotype D). *MafF* silencing in response to si-3 resulted in
316 significant induction of HBV-pgRNA, while administration of si-2 did not yield a similar
317 effect (Fig. 8A, lower panels; $p<0.05$). In all experiments, transcription of pgRNA was
318 inversely associated with expression of *MafF* (Fig. 8B, $p=0.008$); these findings confirmed
319 the role of endogenous MafF with respect to the regulation of HBV-pgRNA transcription.

320 To confirm our earlier findings documenting induction of *MafF* by IL-1β and TNF-α, we
321 treated PXB cells with both cytokines and observed a significant increase in *MafF* mRNA
322 (Fig. 8C, $p<0.05$ for each cytokine).
323
324 ***9. MafF* expression is higher in HBV chronically infected patients with a positive**
325 **correlation to *IL-1β* and *TNF-α* expression**
326 To explore a role for MafF in HBV infection in human subjects, we evaluated data from an
327 open database (67), and found that *MafF* was expressed at significantly higher levels in
328 patients with chronic HBV compared to healthy individuals (Fig. 9A, $p<0.0001$); this was
329 notably the case in patients undergoing immune clearance HBV (Fig. 9B, $p<0.0001$). This
330 result confirmed the induction of *MafF* expression during active inflammation associated
331 with this infection. This observation was strengthened by the demonstration of positive
332 correlations between the levels of *IL-1β* and *TNF-α* transcripts and those encoding *MafF* in
333 the immune clearance patient subset (Fig. 9C, D). Interestingly, no correlations were
334 observed between *MafF* expression and transcripts encoding IFNs (Fig. 9E, F, G, and H).
335 These data suggest that MafF induction associated with chronic HBV disease was unrelated
336 to induction of IFN signaling pathways.
337
338 ## Discussion
339 The intrinsic or innate immune response is mediated by cellular restriction factors.
340 Many of these factors are induced by cytokines (28, 52, 54) and serve to suppress different
341 stages of the viral life cycle, from entry to virion release (5). Several host restriction factors
342 can suppress transcription from DNA virus promoters (53, 63). In this work, we identified
343 MafF as a new host restriction factor that can inhibit both HBV via transcriptional
344 suppression at targeted viral promoter. MafF significantly suppressed HBV core promoter
345 transcription and consequently HBV-pgRNA, core protein and HBV-DNA levels. MafF-KO
346 cells showed a significant increase of HBV core protein with no effect on HBs levels. This
347 can be explained by the major suppressive effect exhibited by MafF on HBV-core promoter

348 in comparison to minimal/no effect of HBV-PreS1, and PreS2 promotors respectively (Fig.
349 2C.)

350 MafF is a member of the small Maf (sMaf) family of transcription factors, a group
351 that includes MafG (19), MafK, and MafF (9). The sMafs are bZIP-type transcription factors
352 that bind to DNA at Maf recognition elements (MAREs). MAREs were initially defined as a
353 13-bp (TGCTGA(G/C)TCAGCA) or 14-bp (TGCTGA(GC/CG)TCAGCA) elements (21,
354 24). However, multiple studies (25, 42, 49) have presented findings suggesting heterogeneity
355 within MARE sequences especially when sMafs heterodimerize with other bZip-type
356 transcription factors. Using the JASPAR database for transcription factor binding sites, we
357 identified a sequence extending from nt 1667 to 1679 (TGGACTCTCAGCG) in the EnhII
358 region of HBV as a potential MafF/bZIP binding region. Although we did not identify the
359 dimerization partner of MafF in this study, the poor alignment at the 5' region of the
360 identified MafF/bZip binding site to the palindromic MARE consensus sequence suggests
361 that MafF binds to this area most probably as a heterodimer with another bZip-type
362 transcription factor. Based on the closer similarity between Bach1 and the identified
363 MafF/bZip binding region (Fig. 5); the previously reported transcription repressor function
364 of sMAFs/Bach1 dimers (56), and the function of MafF as a transcriptional repressor when
365 binding to this area of core promoter; we hypothesize that MafF/Bach1 dimers may be
366 responsible for the transcriptional repression induced by MafF on HBV core promoter
367 activity. Further studies need to be done to confirm this hypothesis and identify the
368 dimerization partner of MafF. Both ChIP and functional analysis confirmed the importance
369 of the interaction between MafF and this specific sequence in HBV core promoter; MafF
370 binding at this core-promoter region results in suppression of the transcriptional activity from
371 HBV core promoter and inhibition of the HBV life cycle. Interestingly, the putative
372 MafF/bZip binding region in the HBV core promoter showed considerable similarity among
373 several HBV genotypes, especially genotypes A, B, and C; MafF-mediated suppression was
374 also observed at core promoters from HBV genotypes A, C, and D. Mutations at the 3' region
375 of the putative MafF/bZip binding site are more frequent in new world HBV genotypes E, F,

376 and G; however, whether these mutations help in evading the suppressive function of MafF
377 and its impact on HBV life cycle still needs to be addressed.
378 Transcription driven from HBV core promoter is controlled by two enhancers,
379 enhancer I (EnhI) and EnhII, the latter overlapping with the core promoter (EnhII/Cp);
380 transcription is also modulated by a negative regulatory element (NRE) (45). Liver-enriched
381 transcription factors, including C/EBPα, HNF-4α, HNF3, FTF/LRH-1, and HLF4, can
382 interact with the EnhII/Cp region and thereby enhance the core promoter activity (15, 47).
383 Negative regulation of HBV core promoter mainly takes place at the NRE, which is located
384 immediately upstream of EnhII (37). Our analysis of the EnhII segment revealed an overlap
385 between MafF and one of the HNF-4α binding sites located between nt 1662 to nt 1674. We
386 identified MafF as a novel negative regulator of EnhII activity that acts via competitive
387 inhibition of HNF-4α binding to the HBV core promoter at this site; we present this
388 mechanism as a plausible explanation for MafF-mediated suppression of HBV infection.
389 The expression levels of sMafs serve as strong determinants of their overall function. An
390 excess of sMafs may increase shift the balance toward transcriptional repression (39). As
391 discussed previously, sMafs dimerize with CNC family proteins Nrf1, Nrf2, Nrf3, Bach1,
392 and Bach2 (38). Furthermore, MARE consensus sites include an embedded canonical AP1
393 motif; as such, some Jun and Fos family factors can also heterodimerize with Maf/CNC
394 proteins. Finally, large Maf proteins are also capable of binding at MARE elements (20, 40).
395 Given the large number of possible homo- and heterodimeric combinations of proteins
396 capable of binding to MAREs, transcriptional responses ranging from subtle to robust can be
397 elicited at a single MARE site (40). Our findings revealed that MafF expression is induced
398 by IL-1β and TNF-α in primary hepatocytes (PXBs) and that this induction was mediated by
399 NF-κB, an inducible transcription factor that is a central regulator of immune and
400 inflammatory responses (29). Both IL-1β and TNF-α have been associated with protection
401 against HBV. For example, a polymorphism in the IL-1β–gene has been linked to disease
402 progression in patients with HBV-related hepatitis (34), while TNF-α expression in
403 hepatocytes induced by HBV (11) has been shown to decrease the extent of HBV persistence
404 (64). We detected higher levels of *MafF* expression in patients with chronic HBV, especially

405 among those in the immune clearance group, compared to healthy individuals. Moreover, we
406 have also reported that IL-1β treatment significantly suppressed HNF-4α interaction with
407 EnhII region of HBV core promoter in response to the induction of MafF expression.
408 Correlation studies in patients' data alone are not conclusive; however, the combination
409 between the in vitro suppressive function of MafF and patients data suggests a possibly
410 important role for MafF with respect to the anti-HBV effects of these cytokines in HBV-
411 infected patients.

412 HBV core promoter regulates the expression of HBV precore and pgRNA transcripts.
413 The precore-RNA serves as the template for the translation of HBV precore protein. HBV-
414 pgRNA is translated into two proteins, HBc (the capsid-forming protein) and pol
415 (polymerase); the HBV-pgRNA also serves as a template for HBV-DNA reverse
416 transcription and viral replication (1). MafF inhibits HBV replication via suppressing the
417 production of HBV-pgRNA, thereby limiting the production of the corresponding
418 replication-associated proteins (core and pol; Fig. 3). We showed here that HBV-pgRNA
419 titers in HBV-infected PXB were higher in cells subjected to MafF silencing; levels of HBV-
420 pgRNA were inversely correlated with MafF mRNA levels (Fig. 7A and B). These data
421 confirmed the importance of endogenous MafF with respect to the regulation of HBV-
422 pgRNA transcription and viral replication. The HBV precore protein is a well-known
423 suppressor of the anti-HBV immune response (35, 60, 66). As such, suppression of HBV
424 precore protein expression may promote a MafF-mediated recovery of the anti-HBV immune
425 response and enhanced viral clearance.

426 To summarize, the results of this work identified MafF as a novel anti-HBV. *MafF*
427 expression was induced by both IL-1β and TNF-α in primary hepatocytes and also in patients
428 with chronic HBV. Furthermore, MafF was shown to play an important role in the
429 suppression of transcription from the HBV core promoter. Further analysis will be needed in
430 order to determine whether the antiviral function of MafF is effective against other DNA
431 viruses as well as its impact on viral evasion mechanisms.

432

433

434 ## Materials and Methods

435 **Cell culture, reagents and establishment of MafF-KO cells**

436 All the cells used in this study were maintained in culture at 37°C and 5% CO_2. HepG2,
437 HepG2-hNTCP-C4, MafF-KO HepG2-hNTCP-C4, and HepAD38.7-Tet cell lines were
438 cultured in Dulbecco's modified Eagle's medium/F-12 (DMEM/F-12) GlutaMAX media
439 (Gibco) as previously described (17). Primary human hepatocytes (Phoenixbio; PXB cells)
440 were cultured as previously described (16). HEK 293FT cells were cultured in DMEM
441 (Sigma) as previously described (2). For the establishment of puromycin resistant-MafF-KO
442 cells, HepG2-hNTCP-C4 cells were co-transfected with MafF CRISPR/Cas9 KO Plasmid
443 (h), sc-411785, and MafF HDR Plasmid (h), sc-411785-HDR, according to manufacturer
444 instruction. Puromycin selection was conducted at 3 μg/mL. Loss of MafF expression was
445 confirmed by immunoblotting. Myrcludex-B was kindly provided by Dr. Stephan Urban at
446 University Hospital Heidelberg and was synthesized by CS Bio (Shanghai, China).

447 **Plasmid Vectors and Construction**

448 An HBV genotype D subtype ayw replicon (58) was obtained from Addgene. HBV Ae
449 (genotype A), HBV D_IND60, and HBV C_JPNAT are 1.24 HBV replicons, which were
450 described previously (55). A MafF expression plasmid (pFN21AB8874) was purchased from
451 Promega. To add a C-terminal HaloTag, the MafF-encoding sequence was subcloned into
452 the PC14K HaloTag vector using the Carboxy Flexi system (Promega). The reporter plasmid
453 for the HBV core promoter mutant was generated by introducing two point mutations
454 (A1676C and C1678A) at the putative MafF binding region (Fig. 4A). Briefly, several rounds
455 of PCR amplification were performed using pGL4.10_Ce_xmut as the template; the resulting
456 products were digested with *Hind*III and *EcoR*I and subcloned into restriction-digested
457 pGL4.10 (Promega). The set of primers used in the construction of the mutated core promoter
458 include forward primers 5'-TCGAGGAATTCGGGTACTTTACCACAGGAAC-3' and 5'-
459 CTTGGACTCTCCGAAATGTCAACG-3' and reverse primers 5'-
460 TTGCCAAGCTTGAACATGAGATGATTAGGC-3' and
461 5'-CGTTGACATTTCGGAGAGTCCAAG-3'. The sequence encoding HNF-4α was
462 amplified from FR_HNF4A2 (Addgene; (57)) by PCR using primers including forward

463 primer, 5'-AGCTAGGATCCACCATGCGACTCTCCAAAACC-3' and reverse primer 5'-
464 GAGTCGAATTCTTACTTGTCGTCATCGTCTTTGTAGTCAGCAACTTGCCCAAAG
465 CG-3'. The resulting amplification product was cloned into pCDNA3.1 (Invitrogen) to yield
466 pcDNA3.1-HNF4A-FLAG. The reporter deletion mutant EnhII/CPΔHNF-4α #2 (Fig. 5A)
467 was constructed using pGL4.10_Ce_xmut as the template and a primer set, including forward
468 primer 5'- TCGAGGGTACCGCCTGTAAATAGACCTATTG-3' and reverse primer 5'-
469 CTAACAAGCTTTCCTCCCCCAACTCCTCCC-3'; the amplification product was
470 subcloned into pGL4.10 using *Hind*III and *Kpn*I restriction enzymes. All constructs were
471 validated by DNA sequencing. Plasmid DNAs used in transfection experiments were purified
472 using the Purelink Plasmid Midi Kit (Invitrogen).

473 **siRNA library**

474 A Silencer Select™ Human Druggable Genome siRNA Library V4 (4397922, Thermo), was
475 used for screening of HepG2-hNTCP-C4 cells infected with the HBV/NL reporter virus. The
476 siRNAs were arrayed in a 96-well format; siRNAs targeting the same genes with different
477 target sequences were distributed across three plates (A, B, and C). The following plates from
478 this siRNA library (2200 human genes) were screened: 1-1, 1-2, 1-3, 1-4, 2-1, 2-2, 2-3, 2-4,
479 3-1, 5-4, 6-2, 6-3, 9-2, 11-3, 11-4, 13-3, 15-1, 15-4, 19-1, 22-2, 25-3, 25-4, 26-1, 26-2, and
480 26-3. Cellular viability was determined using the XTT assay (Roche) according to the
481 manufacturer's instructions. Wells with ≥ 20% loss of cell viability were excluded from
482 further evaluation. Protocols for the preparation of HBV/NL and screening were as described
483 previously (43).

484 **DNA and RNA transfection**

485 Plasmid DNA transfection was performed according to the manufacturer's guidelines, using
486 Lipofectamine 3000 (Invitrogen) for HepG2 cells and Lipofectamine 2000 (Invitrogen) for
487 HEK 293FT cells. Reverse siRNA transfection into HepG2-hNTCP-C4 or HepG2 was
488 performed using Lipofectamine RNAiMAX (Thermo Fisher Scientific); forward siRNA
489 transfection was performed in PXB cells only using Lipofectamine RNAiMAX according to
490 the respective manufacturer's guidelines. Silencer Select™ si-*MafF* (si-1, s24372; si-2,

491 s24371; and si-3, s24370), si-*MafK* (s194858), si-*MafG* (s8419), and the negative control
492 siRNA (#2) were purchased from Thermo Fisher Scientific.

493 **Western blot analysis**

494 Cells were lysed with PRO-PREP protein extraction solution (Intron Biotechnology). Protein
495 samples were separated on a 12% gel via SDS-PAGE. Immunoblotting and protein detection
496 were performed as previously reported (2). Primary antibodies included mouse monoclonal
497 anti-HBc (provided by Dr. Akihide Ryo, Yokohama City University), anti-Halo-tag
498 (Promega), anti-FLAG (M2, Sigma), and anti-actin (Sigma), rabbit polyclonal anti-MafF
499 (Protein Tech), and rabbit monoclonal anti-HNF-4α (Abcam). The band intensities were
500 quantified by ImageJ software (NIH).

501 **HBV and HBV/NL preparation and infection**

502 HBV particles carrying a chimeric HBV virus encoding NanoLuc (NL) were prepared and
503 used as described previously (43). Briefly, HepG2 cells were transfected with a plasmid
504 encoding HBV in which the core region was replaced by a gene encoding NL and a helper
505 plasmid that carried an HBV genome that was defective in packaging. The resulting HBV/NL
506 particles produced NL upon infection. HBV and HBV/NL stocks used in this study were
507 prepared as described previously (17, 43) For infection of HepG2-hNTCP-C4 cells, the cells
508 first were reverse-transfected with *MafF* or negative control siRNAs two days prior to the
509 HBV infection and then infected 2 days later with inoculation of HBV or HBV/NL as
510 described previously (17, 43); the experiment was terminated at 8 days post-infection. For
511 PXB cells, the cells were first infected with HBV; at 3 days post-infection, the cells were
512 transfected with the siRNAs, and the experiment was terminated at 7 days post-infection.

513 **RNA extraction and quantitative real-time PCR**

514 Isolation of total cellular RNA was performed with a RNeasy Mini kit (Qiagen) according to
515 the manufacturer's guidelines and cDNA synthesis was performed using a Superscript VILO
516 cDNA Synthesis Kit (Thermo Fisher Scientific). The relative levels of the *MafF* mRNA was
517 determined using TaqMan 746 Gene Expression Assay primer-probe sets (Applied
518 Biosystems) Hs05026540_g1, expression of *ACTB* (primer-probe set 748 Hs99999903_m1)
519 was used as an internal control for normalization. The quantification of pgRNA, *NTCP*,

520 *HNF-4α, APOA1, and HNF1A* was performed using Power SYBR Green PCR Master Mix
521 (Applied Biosystems); for these transcripts, expression of *GAPDH* was used as an internal
522 control for normalization. Data were expressed as fold change relative to the mean of the
523 control group. The set of primers used in these assays included the Precore forward primer
524 5'-ACTGTTCAAGCCTCCAAGCTGT-3' and reverse primer 5'-
525 GAAGGCAAAAACGAGAGTAACTCCAC-3', *NTCP* forward primer 5′-
526 AGGGAGGAGGTGGCAATCAAGAGTGG-3' and reverse primer 5'-
527 CCGGCTGAAGAACATTGAGGCACTGG-3', *HNF-4α* forward primer 5'-
528 ACTACGGTGCCTCGAGCTGT-3' and reverse primer 5'-
529 GGCACTGGTTCCTCTTGTCT-3'; APOA1 forward primer 5'-
530 CCTTGGGAAAACAGCTAAACC-3', APOA1 reverse primer 5'-
531 CCAGAACTCCTGGGTCACA-3', HNF1A forward primer 5'-
532 CCATCCTCAAAGAGCTGGAG-3', HNF1A reverse primer 5'-
533 TGTTGTGCTGCTGCAGGTA-3', *GAPDH* forward primer 5'-CTTTTGCGTCGCCAG-3'
534 and reverse primer 5'-TTGATGGCAACAATATCCAC-3'.

535 **DNA extraction and cccDNA quantification**

536 For selective extraction of cccDNAs for quantitative PCR, HBV-infected HepG2-hNTCP-
537 C4 cells were harvested and total DNA was extracted using a Qiagen DNA extraction kit
538 according to the manufacturer's instructions but without the addition of Proteinase K as
539 recommended by the concerted harmonization efforts for HBV cccDNA quantification
540 reported in the 2019 International HBV meeting (27). Levels of cccDNA were measured by
541 quantitative real-time PCR (qPCR) using the TaqMan Gene Expression Master Mix (Applied
542 Biosystems), specific primers, and probe as described previously (46). Data were processed
543 as $2^{(-\Delta\Delta Ct)}$ for quantification of cccDNA using chromosomal *GAPDH* DNA sequence (via
544 primer-probe set Hs04420697_g1; Applied Biosystems) as an internal normalization control.

545 **Dual luciferase reporter assay**

546 Firefly luciferase reporter plasmids carrying the entire HBV core promoter (nt 900 to 1817),
547 Enh1/X promoter (nt 950 to 1373), preS1 promoter (nt 2707 to 2847), or preS2/S promoter
548 (nt 2937 to 3204) were constructed as previously reported (8). HepG2 cells were co-

549 transfected with the firefly reporter vectors and the *Renilla* luciferase plasmid pRL-TK
550 (Promega) as an internal control. At 48 h post-transfection, the cells were lysed and luciferase
551 activities were measured using the Dual-Luciferase Reporter Assay System (Promega). For
552 experiments involving IL-1β, cells were treated for 3 h with IL-1β (1 ng/ml) at 48 h post-
553 transfection followed by evaluation of dual luciferase activity.
554
555 **Quantification of HBs and HBe antigens**
556 Cell supernatants were harvested and an ELISA was performed as described previously for
557 HBs (61) whereas for HBe, Enzygnost HBe monoclonal, Siemens was used according to the
558 manufacturer's instructions.
559
560 **Indirect Immunofluorescence Analysis**
561 Indirect immunofluorescence analysis was performed essentially as described previously
562 (61). After fixation with 4% paraformaldehyde and permeabilization with 0.3% Triton X-
563 100, an anti-HBc antibody (HBP-023-9, Austral Biologicals) was used as the primary
564 antibody.
565 **Southern blotting assay**
566 HepG2 cells were co-transfected with MafF-encoding or control vectors together with the
567 HBV ayw plasmid both with or without 5 μM entecavir (Sigma) as a control. At 3 days post-
568 transfection, core-associated DNA was isolated from intracellular viral capsids as described
569 previously (50). Southern blot analysis to detect HBV-DNAs was performed also as
570 described previously (2) For the detection of HBV cccDNA by southern blotting, the HBV
571 cccDNA was extracted through protein free Hirt DNA extraction. Hirt DNA was heated at
572 95ºC for 10 minutes to allow the denaturation of DP-rcDNA and dsDNA into single stranded
573 DNA. The heat-treated samples were then digested with EcoRI to linearize the cccDNA. The
574 Hirt DNA samples were then separated by agarose gel at 25 volts for 12 hours. After southern
575 blot transfer, the DNA was hybridized with DIG Easy Hyb (Roche-11603558001) and
576 detected with DIG wash and block buffer set (Roche-11585762001).

577 **Chromatin Immunoprecipitation (ChIP) assay**

578 293FT cells were co-transfected with a MafF expression plasmid together a reporter plasmid
579 harboring either the WT or mutated core promoter (substitution mutations in MARE) at a 4:1
580 ratio for assessment of the interactions between MafF and HBV core promoter. In other
581 experiments, 293FT cells were co-transfected with plasmids encoding FLAG-tagged
582 EnhII/CPΔHNF-4α#2, and a MafF expression plasmid (or empty vector) at a 1: 2 ratio for
583 assessment of competitive binding of MafF and HNF-4α. Rabbit monoclonal anti-HNF-4α
584 (Abcam, EPR16885) was used for IP. To elucidate the effect of IL-1β on MafF and HNF-4α
585 competition, HepG2 cells were transfected with anti-MafF si-3 and plasmid encoding
586 EnhII/CPΔHNF-4α#2. At 48 h post-transfection IL-1β was added to the culture medium
587 (1ng/mL) for 3 hours. ChIP was carried out using a Magna ChIP G kit (Millipore) according
588 to the manufacturer's instructions. Anti-HNF-4α Rabbit monoclonal antibody (Abcam) was
589 used for IP.

590

591 **Cytokine treatment and NF-κB inhibitors**

592 Responses to IL-1β and TNF-α (R&D Systems) were evaluated in HepG2 cells (at 1 ng/ml
593 and 10 ng/ml, respectively) and in PXB cells (both at 10 ng/ml) after 1, 3, and 6 h. For the
594 experiments involving NF-κB inhibitors, Bay11-7082 and BMS-345541 (both from Tocris)
595 were added to final concentrations of 10 μM and 5 μM, respectively. HepG2 cells were
596 pretreated for 1 h with each inhibitor followed by the addition of 1 ng/ml IL-1β (for 1 and 3
597 h) or 10 ng/ml TNF-α (for 1 h). All experiments included phosphate-buffered saline (PBS)
598 as a diluent control for the cytokines and dimethyl sulfoxide (DMSO) as the diluent control
599 for the NF-κB inhibitors.

600

601 **Database**

602 Transcriptional profiling of the patients with chronic HBV (CHB) (GSE83148) and of HBV
603 patients with immune tolerance and those undergoing HBV clearance (GSE65359) were
604 identified in the Gene Expression Omnibus public database. Expression data for *MafF* and
605 for genes encoding cytokines *IL-1β, TNF-α, IFNA1, IFN-β1, IFNL1, and IFNL2* were

606 extracted by GEO2R. HBx sequences (n = 10,846) were collected from HBVdb (13). For
607 each genotype, nucleotide sequences were aligned by using MAFFT version 7.471 (22).
608 Multiple sequence alignments of the MARE region were depicted using WebLogo version
609 2.8 (7). The overall height of the stack indicates the conservation at the site while the relative
610 frequency of each nucleic acid is shown as the height of the characters within the stack.

611

612 **Statistical analysis**

613 The data were analyzed with algorithms included in Prism (v. 5.01; GraphPad Software, San
614 Diego, CA). Tests for normal distribution of the data were performed. Two-tailed unpaired t
615 tests, and Mann-Whitney U tests were used for statistical analysis of parametric and non-
616 parametric data, respectively. The correlation coefficients were determined by Pearson or
617 Spearman correlation analysis of parametric and non-parametric data, respectively. Values
618 of $p \leq 0.05$ were considered statistically significant.

619

620 **Acknowledgments**

621 Ibrahim MK was the recipient of a JSPS postdoctoral fellowship. This study was supported
622 by a Grant-In-Aid for JSPS Fellows (18F18098), and for Scientific Research (19K07586),
623 and grants from the Research Program on Hepatitis from the Japan Agency for Medical
624 Research and Development (AMED; 19fk0310104j0903, 19fk0310103j0303,
625 19fk0310109h0003, and 19fk0310109j0403). Myrcludex-B, a pre-S1 lipopeptide, was kindly
626 provided by Dr. Stephan Urban at the University Hospital Heidelberg. We gratefully
627 acknowledge Dr. Akihide Ryo (Yokohama City University School of Medicine) for the kind
628 gift of the anti-HBV core antibody, Dr. Takayuki Murata (Fujita Health University), Dr. Iwao
629 Kukimoto, Miss Yingfang Li, Mr. Sameh A. Gad, Dr. Xin Zheng, and Dr. Haruka Kudo
630 (NIID) for productive discussion, criticism, and technical support. We are also very grateful
631 to Dr. Haitao Guo (University of Pittsburgh) for his great educational support that enabled
632 us to detect HBV-cccDNA.

633

634

635 ## Figure Legends

636 **Figure 1. MafF suppresses HBV infection**

637 **A.** A schematic diagram showing the experimental approach used to screen the siRNA library.
638 **B.** HepG2-hNTCP-C4 cells were transfected with control, *NTCP*, or *MafF*-targeting siRNAs
639 (si-1, si-2, and si-3); two days later, transfected cells were infected with the HBV/NL reporter
640 virus. At day 8 post-infection, luciferase assays were performed, and NanoLuc activity was
641 measured and plotted. **C.** HepG2 cells were transfected with control or *MafF*-targeting
642 siRNAs (si-1, si-2, and si-3); total protein was extracted after two days. Expression of MafF
643 (upper panel) and actin (control; lower panel) was analyzed by immunoblotting with their
644 respective antibodies. **D.** HepG2 cells were transfected with control or *MafF*-targeting siRNA
645 (si-3); total protein was extracted after ten days. Expression of MafF (upper panel) and actin
646 (control; lower panel) was analyzed by immunoblotting with their respective antibodies. All
647 assays were performed in triplicate and included three independent experiments. Data are
648 presented as mean±standard deviation (SD); $^{**}p<0.01$, $^{***}p<0.001$, $^{****}p< 0.0001$; NS, not
649 significant

650

651 **Figure 2. MafF suppresses the transcriptional activity of the HBV core promoter.**

652 **A.** HepG2-hNTCP-C4 cells were transfected with control or *MafF*-targeting siRNA (si-3).
653 Two days after transfection, the transfected cells were infected with HBV at 12,000 genomic
654 equivalents (GEq) per cell. Eight days later, the cells were harvested, DNA was extracted,
655 and cccDNA was quantified by real-time PCR. The data were normalized to the levels of
656 endogenous *GAPDH DNA* and are presented as fold change relative to control siRNA-
657 transfected cells. **B.** HepG2-hNTCP-C4 cells were transfected with control or *MafF*-targeting
658 siRNA (si-3). Two days after transfection, the transfected cells were infected with HBV at
659 12,000 GEq per cell. Eight days later, the cells were harvested, HIRT purification of DNA
660 was performed, and cccDNA was visualized by southern blotting assay. C. HepG2 cells (left
661 panel) were co-transfected with a MafF expression vector or empty vector (control) together
662 with firefly luciferase reporter plasmids with HBV promoters (core, X, S1, and S2) and the
663 pRL-TK control plasmid encoding *Renilla* luciferase. Two days after transfection, the cells

were harvested and evaluated by dual luciferase assay. HepG2 cells (right panel) were transfected with control or *MafF*-targeting siRNA (si-3); 24 hours later, the cells were transfected with firefly luciferase reporter-HBV core promoter vector and the pRL-TK plasmid encoding *Renilla* luciferase. Two days later, the cells were lysed and evaluated by dual luciferase assay. For panel C, firefly luciferase data were normalized to *Renilla* luciferase levels; relative light units (RLUs) for firefly luciferase were plotted as fold differences relative to the levels detected in the control groups. All assays were performed in triplicate and included three independent experiments; data are presented as mean±SD. ****$p<0.0001$; NS, not significant.

Figure 3. MafF suppresses HBV life cycle.

A. HepG2 cells were transfected with empty (control) or MafF expression vector together with expression vectors encoding HBV genotypes A and D. Two days later, the cells were harvested and the pgRNA expression was quantified by real-time RT-PCR. The data were normalized to the expression of *GAPDH* and are shown as the fold change relative to control plasmid-transfected cells. **B–D:** HepG2 cells were transfected with empty (control) or MafF expression vectors together with an expression plasmid encoding HBV genotype D **(B)** At 2 days post-transfection, HBeAg in the cell culture supernatants were quantified by ELISA. **(C)** The intracellular levels of HBV core protein (upper left panel) and actin (loading control; lower left panel) were evaluated by immunoblotting; the intensities of the bands (right panel) were quantified by ImageJ software. **(D)** At 3 days post-transfection, the levels of intracellular core-associated DNA were determined by southern analysis; transfected cells treated with 10 μM entecavir were used as controls.

Data are presented as fold differences relative to the control plasmid-transfected cells. All assays were performed in triplicate and include results from three independent experiments; data are presented as mean±SD; *$p<0.05$, ****$p<0.0001$.

693 **Fig. 4. Enhanced expression of HBc in MafF-KO cells.**

694 A. HepG2-hNTCP-C4 cells were co-transfected with MAfF CRISPR/Cas9 KO Plasmid (h),
695 sc-411785, and MAfF HDR Plasmid (h), sc-411785-HDR. Puromycin selection was
696 conducted at 3μg/mL for 2 weeks. 11 isolated colonies were picked and scaled up. MafF
697 expression was detected by immunoblotting, as positive and negative controls, we used WT
698 (HepG2-hNTCP-C4) cells, and si-3 treated HepG2-hNTCP-C4 cells respectively. B. HepG2-
699 hNTCP-C4, MafF-KO-8, and MafF-KO-11 cells were infected with HBV/NL reporter virus.
700 Cells were pretreated with or without 1 μM Myrcludex-B or vehicle (DMSO) for 3 h before
701 infection. At day 8 post-infection, luciferase assays were performed, and NanoLuc activity
702 was measured and plotted as fold-difference relative to the mean luciferase levels in HepG2-
703 hNTCP-C4 cells. C. HepG2-hNTCP-C4, or MafF-KO-11 cells were infected with HBV
704 (6000 GEq/cell), at 12 days post-infection, HBc in the cells was detected by
705 immunofluorescent (left panel) and fluorescent intensity was plotted as fold-difference
706 relative to its mean levels in HBV-infected HepG2-hNTCP-C4 cells. D. HepG2-hNTCP-C4,
707 or MafF-KO-11 cells were infected with HBV (6000 GEq/cell). Cells were pretreated with
708 or without 1 μM Myrcludex-B or vehicle (DMSO) for 3 h before infection. After 12 days from
709 infection, HBsAg in the cell culture supernatants was measured and plotted as fold-difference
710 relative to the its mean levels in the supernatant of HBV-infected HepG2-hNTCP-C4 cells.
711 All assays were performed in triplicate and include results from three independent
712 experiments; data are presented as mean±SD; $^{**}p<0.01$, $^{***}p<0.001$.

713

714

715 **Figure 5. Physical interaction of MafF with HBV core promoter is required for**
716 **transcriptional repression.**

717 **A.** A schematic representation of the putative MafF/bZIP binding region within enhancer 2
718 (EnhII) of the HBV core promoter from HBV genotype C. A mutant construct was prepared
719 by introducing two point mutations (A1676C and C1678A) into the MARE sequence
720 identified in the wild-type (WT) core promoter. B**.** HepG2 cells were co-transfected with
721 mock (left panel) or a MafF expression plasmid (right panel) along with an HBV core

722 promoter (WT or mutant)-reporter plasmid and pRL-TK encoding *Renilla* luciferase. At two
723 days post-transfection, a dual luciferase assay was performed; firefly luciferase data were
724 normalized relative to *Renilla* luciferase levels, and RLUs for firefly luciferase are plotted as
725 fold differences relative to activity in the control group. **C.** 293FT cells were transfected with
726 either the WT or mutant HBV core promoter-luciferase reporter plasmid together with a
727 MafF expression plasmid (at a ratio 1:4). At two days post-transfection, cell lysates were
728 collected; two aliquots (1/10 volume each) were removed from each sample. One aliquot was
729 used for the detection of MafF protein (Input) and actin (loading control) by immunoblotting
730 (upper and middle right panels); the second aliquot was used for DNA extraction and
731 detection of HBV core promoter (Input) by real-time PCR. The remaining cell lysates (each
732 8/10 of the original volume) were subjected to ChIP assay using either isotype control
733 antibody (rabbit IgG) or rabbit anti-MafF IgG to detect MafF. Following
734 immunoprecipitation (IP), 1/10 volume of each IP sample was analyzed by immunoblotting
735 for MafF (lower right panel); each remaining IP sample was subjected to DNA extraction
736 and real-time PCR assay in order to detect associated HBV core promoter DNA. The fraction
737 of core promoter DNA immunoprecipitated compared to the input value was determined by
738 real-time PCR and was expressed as percent of input (% of input) and as the fold enrichment
739 over the fraction of *GAPDH* DNA immunoprecipitated. D. A schematic representation of the
740 putative MafF/bZIP binding region within enhancer 2 (EnhII) of the HBV core promoter
741 from different HBV genotypes. 10,846 HBx sequences were collected from HBVdb, The
742 multiple sequence alignments of the MARE region were depicted by using WebLogo version
743 2.8. The overall height of the stack indicates the conservation at the site, while the relative
744 frequency of each nucleic acid is shown as the height of the characters within the stack. The
745 assays of panel B and C were performed in triplicate and include data from three independent
746 experiments. Data are presented as mean±SD; *$p<0.05$, **$p<0.01$, ****$p<0.0001$.
747
748 **Figure 6. MafF competes with HNF-4α for binding to the HBV core promoter.**
749 **A.** A schematic representation of the enhancer 2 (EnhII) and the basal HBV core promoter
750 (Cp; nt 1591-1798) featuring the putative MafF binding region (nt 1667–1679) and the two

751 HNF-4α binding sites HNF-4α#1 (nt 1662–1674) and HNF-4α#2 (nt 1757–1769). A deletion
752 mutant construct (EnhII/Cp Δ HNF-4α#2, nt 1591–1750) was prepared to eliminate HNF-
753 4α#2. **B.** 293FT cells were co-transfected with the EnhII/Cp Δ HNF-4α#2-luciferase reporter
754 plasmid, a FLAG-tagged HNF-4α expression plasmid, and a MafF (or control) expression
755 plasmid at a ratio of 1:1:2. At two days post-transfection, cell lysates were collected and two
756 aliquots (1/10 volume each) were removed from each sample. One aliquot was used for the
757 detection of HNF-4α protein (Input) and actin (loading control) by immunoblotting (lower
758 panel); the second aliquot was used for DNA extraction and detection of HBV core promoter
759 (Input) by real-time PCR. The remaining cell lysates (each 4/10 of the original volume) were
760 subjected to ChIP assay using isotype control antibody (rabbit IgG) or rabbit anti-HNF-4α
761 IgG to precipitate FLAG-tagged HNF-4α. Following immunoprecipitation (IP), 1/5 volume
762 of each IP sample was analyzed by immunoblotting to detect HNF-4α (lower panel) and each
763 remaining IP sample was subjected to DNA extraction and real-time PCR assay for the
764 detection of associated HBV core promoter DNA. The fraction of core promoter DNA
765 immunoprecipitated compared to the input value was determined by real-time PCR and was
766 expressed as percent of input (% of input) (upper left panel) and as the fold enrichment (upper
767 right panel) over the fraction of *GAPDH* DNA immunoprecipitated. **C. Left panel:** HepG2
768 cells were transfected with empty vector (control) or MafF expression vector. After 24 h or
769 48 h, total RNA was extracted and *HNF-4α* expression was quantified by real-time RT-PCR.
770 The data were normalized to *GAPDH* expression and are presented as fold differences
771 relative to the control cells. **Right panel:** HepG2 cells were transfected with control or *MafF*-
772 targeting siRNA (si-3) and *HNF-4α* expression was evaluated 48 h later as noted just above.
773 **D.** HepG2 cells were transfected with control or *MafF*-targeting siRNA (si-3), and *HNF1A*
774 and *ApoA-1* expression was evaluated after 48 h as previously mentioned . All assays were
775 performed in triplicate and data are presented from three independent experiments. Data are
776 presented as mean±SD; *p<0.05, **p<0.01; NS, not significant.
777
778 **Figure 7. IL-1β and TNF-α induce MafF expression via NF-κB-mediated signaling**

779 **A.** HepG2 cells were treated with IL-1β (1 ng/ml), TNF-α (10 ng/ml), or PBS (diluent
780 control) for the times as indicated (hours). The cells then were lysed, total cellular RNA was
781 extracted, and *MafF* mRNA was quantified by real-time RT-PCR. The data were normalized
782 to the expression of *ACTB* and are shown as the fold change relative to the mean of the control
783 group. **B.** HepG2 cells were treated for 24 h with IL-1β, TNF-α, or PBS control as in A.; the
784 cells then were harvested and total protein was extracted. Expression of MafF (upper panel)
785 and actin (the loading control; lower panel) was analyzed by immunoblotting. **C, D, and E.**
786 HepG2 cells were pretreated with NF-κB inhibitors Bay11-7082**,** BMS-345541, or DMSO
787 (diluent control) for 1 h and then treated with 1 ng/ml IL-1β (**C, D**), 10 ng TNF-α (**E**) or PBS
788 (control) for 1 and 3 h. Expression of MafF was quantified by real-time RT-PCR and were
789 normalized to the expression of the *ACTB* and shown as the fold change relative to the mean
790 of the control group. **F.** HepG2 cells were transfected with the anti-MafF si-3 and EnhII/Cp
791 ΔHNF-4α#2-luciferase reporter plasmid. At two days post-transfection, cells were treated
792 with IL-1β (1 ng/mL) or mock for 3 hours, then cell lysates were collected and two aliquots
793 (1/10 volume each) were removed from each sample. One aliquot was used for the detection
794 of HNF-4α protein (Input) and actin (loading control) by immunoblotting (lower panel); the
795 second aliquot was used for DNA extraction and detection of HBV core promoter (Input) by
796 real-time PCR. The remaining cell lysates (each 4/10 of the original volume) were subjected
797 to ChIP assay using isotype control antibody (rabbit IgG) or rabbit anti-HNF-4α IgG to
798 precipitate endogenous HNF-4α. Following immunoprecipitation (IP), 1/5 volume of each IP
799 sample was analyzed by immunoblotting to detect HNF-4α (lower panel) and each remaining
800 IP sample was subjected to DNA extraction and real-time PCR assay for the detection of
801 associated EnhII/Cp ΔHNF-4α#2 DNA. The fraction of EnhII/Cp ΔHNF-4α#2 DNA
802 immunoprecipitated compared to the input value was determined by real-time PCR and was
803 expressed as percent of input (% of input) (upper left panel) and as the fold enrichment (upper
804 right panel) over the fraction of *GAPDH* DNA immunoprecipitated.

805 All assays were performed in triplicate and including the results from three (panels A, B, and
806 C) or two (D, E and F) independent experiments. Data are presented as mean±SD; *p<0.05,
807 ***p*<0.01, ****p*< 0.0001.
808
809 **Figure 8. MafF suppresses HBV infection in primary human hepatocytes (PXB cells).**
810 **A.** Primary hepatocytes (PXB cells) were infected with HBV virions at 5,000 GEq per cell.
811 After 3 days, the cells were transfected with control or *MafF*-targeting siRNAs (si-2 and si-
812 3); at 4 days after transfection, total RNA was extracted. **Upper panel:** *MafF* expression
813 level was quantified by real-time RT-PCR and normalized to the expression of *ACTB*. **Lower**
814 **panel:** Levels of pgRNA were quantified by real-time RT-PCR using a standard curve
815 quantification method. Data are presented as fold differences relative to the control siRNA-
816 transfected cells. **B.** Correlation between expression of *MafF* mRNA and pgRNA in HBV-
817 infected and siRNA-transfected PXB cells as described in A. **C.** Primary hepatocytes (PXB)
818 cells were treated with IL-1β (at 10 ng/ml), TNF-α (at 10 ng/ml), or PBS (diluent control) for
819 the times indicated (hours). The cells then were lysed, total cellular RNA was extracted, and
820 *MafF* mRNA was quantified by real-time RT-PCR. The data were normalized to the
821 expression of *ACTB* and are shown as the fold change relative to the mean of the control
822 group. D. MafF mRNA expression detected by RNA sequencing in single primary hepatocyte
823 (PXB) infected with HBV. All assays were performed in triplicate and include data from two
824 independent experiments. Data are presented as mean±SD; **p*<0.05, ***p*<0.01; NS, not
825 significant
826
827 **Figure 9. *MafF* expression is increased in patients with chronic HBV infections and is**
828 **positively correlated to expression of *IL-1β* and *TNF-α* mRNAs**
829 **A.** *MafF* mRNA levels in the liver tissue of patients with chronic hepatitis B infection (CHB;
830 n=122) and healthy subjects (n=6, GSE83148). **B.** *MafF* mRNA levels in the liver tissue of
831 immune-tolerant (n=22) and immune clearance (n=50) HBV-infected patients (GSE65359).
832 **C.-H.** Correlations between the expression of mRNAs encoding *MafF* and **C.** *IL-1β*, **D.** *TNF-*

833 α, **E**. *IFN-β1*, **F.** *IFNA1*, **G**. *IFNL1*, and **H**. *IFNL2* in liver tissue of patients undergoing
834 immune clearance. In panels A and D, data are presented as the mean±SD; ****p<0.0001.
835
836
837
838

839 1. **Abraham, T. M., and D. D. Loeb.** 2007. The topology of hepatitis B virus pregenomic RNA
840 promotes its replication. J Virol **81:**11577-84.
841 2. **Aly, H. H., J. Suzuki, K. Watashi, K. Chayama, S. Hoshino, M. Hijikata, T. Kato, and T. Wakita.**
842 2016. RNA Exosome Complex Regulates Stability of the Hepatitis B Virus X-mRNA Transcript
843 in a Non-stop-mediated (NSD) RNA Quality Control Mechanism. J Biol Chem **291:**15958-74.
844 3. **Amini-Bavil-Olyaee, S., Y. J. Choi, J. H. Lee, M. Shi, I. C. Huang, M. Farzan, and J. U. Jung.**
845 2013. The antiviral effector IFITM3 disrupts intracellular cholesterol homeostasis to block
846 viral entry. Cell Host Microbe **13:**452-64.
847 4. **Bartenschlager, R., and H. Schaller.** 1992. Hepadnaviral assembly is initiated by polymerase
848 binding to the encapsidation signal in the viral RNA genome. EMBO J **11:**3413-20.
849 5. **Chemudupati, M., A. D. Kenney, S. Bonifati, A. Zani, T. M. McMichael, L. Wu, and J. S.**
850 **Yount.** 2019. From APOBEC to ZAP: Diverse mechanisms used by cellular restriction factors
851 to inhibit virus infections. Biochim Biophys Acta Mol Cell Res **1866:**382-394.
852 6. **Chen, G., C. H. Liu, L. Zhou, and R. M. Krug.** 2014. Cellular DDX21 RNA helicase inhibits
853 influenza A virus replication but is counteracted by the viral NS1 protein. Cell Host Microbe
854 **15:**484-93.
855 7. **Crooks, G. E., G. Hon, J. M. Chandonia, and S. E. Brenner.** 2004. WebLogo: a sequence logo
856 generator. Genome Res **14:**1188-90.
857 8. **Deng, L., X. Gan, M. Ito, M. Chen, H. H. Aly, C. Matsui, T. Abe, K. Watashi, T. Wakita, T.**
858 **Suzuki, T. Okamoto, Y. Matsuura, M. Mizokami, I. Shoji, and H. Hotta.** 2019. Peroxiredoxin
859 1, a Novel HBx-Interacting Protein, Interacts with Exosome Component 5 and Negatively
860 Regulates Hepatitis B Virus (HBV) Propagation through Degradation of HBV RNA. J Virol **93**.
861 9. **Fujiwara, K. T., K. Kataoka, and M. Nishizawa.** 1993. Two new members of the maf
862 oncogene family, mafK and mafF, encode nuclear b-Zip proteins lacking putative trans-
863 activator domain. Oncogene **8:**2371-80.
864 10. **Gilbert, S., L. Galarneau, A. Lamontagne, S. Roy, and L. Belanger.** 2000. The hepatitis B virus
865 core promoter is strongly activated by the liver nuclear receptor fetoprotein transcription
866 factor or by ectopically expressed steroidogenic factor 1. J Virol **74:**5032-9.
867 11. **Gonzalez-Amaro, R., C. Garcia-Monzon, L. Garcia-Buey, R. Moreno-Otero, J. L. Alonso, E.**
868 **Yague, J. P. Pivel, M. Lopez-Cabrera, E. Fernandez-Ruiz, and F. Sanchez-Madrid.** 1994.
869 Induction of tumor necrosis factor alpha production by human hepatocytes in chronic viral
870 hepatitis. J Exp Med **179:**841-8.
871 12. **Gripon, P., I. Cannie, and S. Urban.** 2005. Efficient inhibition of hepatitis B virus infection by
872 acylated peptides derived from the large viral surface protein. J Virol **79:**1613-22.
873 13. **Hayer, J., F. Jadeau, G. Deleage, A. Kay, F. Zoulim, and C. Combet.** 2013. HBVdb: a
874 knowledge database for Hepatitis B Virus. Nucleic Acids Res **41:**D566-70.

875 14. **Hirsch, R. C., J. E. Lavine, L. J. Chang, H. E. Varmus, and D. Ganem.** 1990. Polymerase gene
876 products of hepatitis B viruses are required for genomic RNA packaging as wel as for reverse
877 transcription. Nature **344:**552-5.
878 15. **Ishida, H., K. Ueda, K. Ohkawa, Y. Kanazawa, A. Hosui, F. Nakanishi, E. Mita, A. Kasahara,**
879 **Y. Sasaki, M. Hori, and N. Hayashi.** 2000. Identification of multiple transcription factors, HLF,
880 FTF, and E4BP4, controlling hepatitis B virus enhancer II. J Virol **74:**1241-51.
881 16. **Ishida, Y., C. Yamasaki, A. Yanagi, Y. Yoshizane, K. Fujikawa, K. Watashi, H. Abe, T. Wakita,**
882 **C. N. Hayes, K. Chayama, and C. Tateno.** 2015. Novel robust in vitro hepatitis B virus
883 infection model using fresh human hepatocytes isolated from humanized mice. Am J Pathol
884 **185:**1275-85.
885 17. **Iwamoto, M., K. Watashi, S. Tsukuda, H. H. Aly, M. Fukasawa, A. Fujimoto, R. Suzuki, H.**
886 **Aizaki, T. Ito, O. Koiwai, H. Kusuhara, and T. Wakita.** 2014. Evaluation and identification of
887 hepatitis B virus entry inhibitors using HepG2 cells overexpressing a membrane transporter
888 NTCP. Biochem Biophys Res Commun **443:**808-13.
889 18. **Kannan, M. B., V. Solovieva, and V. Blank.** 2012. The small MAF transcription factors MAFF,
890 MAFG and MAFK: current knowledge and perspectives. Biochim Biophys Acta **1823:**1841-6.
891 19. **Kataoka, K., K. Igarashi, K. Itoh, K. T. Fujiwara, M. Noda, M. Yamamoto, and M. Nishizawa.**
892 1995. Small Maf proteins heterodimerize with Fos and may act as competitive repressors of
893 the NF-E2 transcription factor. Mol Cell Biol **15:**2180-90.
894 20. **Kataoka, K., M. Nishizawa, and S. Kawai.** 1993. Structure-function analysis of the maf
895 oncogene product, a member of the b-Zip protein family. Journal of Virology **67:**2133-2141.
896 21. **Kataoka, K., M. Noda, and M. Nishizawa.** 1994. Maf nuclear oncoprotein recognizes
897 sequences related to an AP-1 site and forms heterodimers with both Fos and Jun. Mol Cell
898 Biol **14:**700-12.
899 22. **Katoh, K., and D. M. Standley.** 2013. MAFFT multiple sequence alignment software version
900 7: improvements in performance and usability. Mol Biol Evol **30:**772-80.
901 23. **Katsuoka, F., and M. Yamamoto.** 2016. Small Maf proteins (MafF, MafG, MafK): History,
902 structure and function. Gene **586:**197-205.
903 24. **Kerppola, T. K., and T. Curran.** 1994. A conserved region adjacent to the basic domain is
904 required for recognition of an extended DNA binding site by Maf/Nrl family proteins.
905 Oncogene **9:**3149-58.
906 25. **Kimura, M., T. Yamamoto, J. Zhang, K. Itoh, M. Kyo, T. Kamiya, H. Aburatani, F. Katsuoka,**
907 **H. Kurokawa, T. Tanaka, H. Motohashi, and M. Yamamoto.** 2007. Molecular basis
908 distinguishing the DNA binding profile of Nrf2-Maf heterodimer from that of Maf
909 homodimer. J Biol Chem **282:**33681-90.
910 26. **Krause-Kyora, B., J. Susat, F. M. Key, D. Kuhnert, E. Bosse, A. Immel, C. Rinne, S. C. Kornell,**
911 **D. Yepes, S. Franzenburg, H. O. Heyne, T. Meier, S. Losch, H. Meller, S. Friederich, N.**
912 **Nicklisch, K. W. Alt, S. Schreiber, A. Tholey, A. Herbig, A. Nebel, and J. Krause.** 2018.
913 Neolithic and medieval virus genomes reveal complex evolution of hepatitis B. Elife **7**.
914 27. **Lena Allweiss, M. Y., Barbara Testoni, Julie Lucifora, Chunkyu Ko, Bingqian Qu, Dieter**
915 **Glebe, Elena S. kim, Mark Lutgehetmann, Stephan Urban, Guofeng Cheng, William**
916 **Delaney, Massimo Levrero, Ulrike Protzer, Fabien Zoulim, Haitao Guo, Maura Dandri.** 2019.
917 Final results of the concerted harmonization efforts for HBV cccDNA quantification, 2019
918 International HBV Meeting, Melbourne, Australia.

919 28. **Liang, G., G. Liu, K. Kitamura, Z. Wang, S. Chowdhury, A. M. Monjurul, K. Wakae, M. Koura,**
920 **M. Shimadu, K. Kinoshita, and M. Muramatsu.** 2015. TGF-beta suppression of HBV RNA
921 through AID-dependent recruitment of an RNA exosome complex. PLoS Pathog
922 **11:**e1004780.
923 29. **Liu, T., L. Zhang, D. Joo, and S. C. Sun.** 2017. NF-kappaB signaling in inflammation. Signal
924 Transduct Target Ther **2**.
925 30. **Lopez-Cabrera, M., J. Letovsky, K. Q. Hu, and A. Siddiqui.** 1991. Transcriptional factor C/EBP
926 binds to and transactivates the enhancer element II of the hepatitis B virus. Virology
927 **183:**825-9.
928 31. **Massrieh, W., A. Derjuga, F. Doualla-Bell, C. Y. Ku, B. M. Sanborn, and V. Blank.** 2006.
929 Regulation of the MAFF transcription factor by proinflammatory cytokines in myometrial
930 cells. Biol Reprod **74:**699-705.
931 32. **Meurs, E. F., Y. Watanabe, S. Kadereit, G. N. Barber, M. G. Katze, K. Chong, B. R. Williams,**
932 **and A. G. Hovanessian.** 1992. Constitutive expression of human double-stranded RNA-
933 activated p68 kinase in murine cells mediates phosphorylation of eukaryotic initiation factor
934 2 and partial resistance to encephalomyocarditis virus growth. J Virol **66:**5805-14.
935 33. **Meyerson, N. R., L. Zhou, Y. R. Guo, C. Zhao, Y. J. Tao, R. M. Krug, and S. L. Sawyer.** 2017.
936 Nuclear TRIM25 Specifically Targets Influenza Virus Ribonucleoproteins to Block the Onset
937 of RNA Chain Elongation. Cell Host Microbe **22:**627-638 e7.
938 34. **Migita, K., Y. Maeda, S. Abiru, M. Nakamura, A. Komori, S. Miyazoe, K. Nakao, H.**
939 **Yatsuhashi, K. Eguchi, and H. Ishibashi.** 2007. Polymorphisms of interleukin-1beta in
940 Japanese patients with hepatitis B virus infection. J Hepatol **46:**381-6.
941 35. **Mitra, B., J. Wang, E. S. Kim, R. Mao, M. Dong, Y. Liu, J. Zhang, and H. Guo.** 2019. Hepatitis
942 B Virus Precore Protein p22 Inhibits Alpha Interferon Signaling by Blocking STAT Nuclear
943 Translocation. J Virol **93**.
944 36. **Mogilenko, D. A., E. B. Dizhe, V. S. Shavva, I. A. Lapikov, S. V. Orlov, and A. P.**
945 **Perevozchikov.** 2009. Role of the nuclear receptors HNF4 alpha, PPAR alpha, and LXRs in
946 the TNF alpha-mediated inhibition of human apolipoprotein A-I gene expression in HepG2
947 cells. Biochemistry **48:**11950-60.
948 37. **Moolla, N., M. Kew, and P. Arbuthnot.** 2002. Regulatory elements of hepatitis B virus
949 transcription. J Viral Hepat **9:**323-31.
950 38. **Motohashi, H., F. Katsuoka, J. A. Shavit, J. D. Engel, and M. Yamamoto.** 2000. Positive or
951 negative MARE-dependent transcriptional regulation is determined by the abundance of
952 small Maf proteins. Cell **103:**865-75.
953 39. **Motohashi, H., T. O'Connor, F. Katsuoka, J. D. Engel, and M. Yamamoto.** 2002. Integration
954 and diversity of the regulatory network composed of Maf and CNC families of transcription
955 factors. Gene **294:**1-12.
956 40. **Motohashi, H., J. A. Shavit, K. Igarashi, M. Yamamoto, and J. D. Engel.** 1997. The world
957 according to Maf. Nucleic Acids Res **25:**2953-59.
958 41. **Nassal, M.** 2015. HBV cccDNA: viral persistence reservoir and key obstacle for a cure of
959 chronic hepatitis B. Gut **64:**1972-84.
960 42. **Ney, P. A., B. P. Sorrentino, C. H. Lowrey, and A. W. Nienhuis.** 1990. Inducibility of the HS
961 II enhancer depends on binding of an erythroid specific nuclear protein. Nucleic Acids Res
962 **18:**6011-7.

963 43. **Nishitsuji, H., S. Ujino, Y. Shimizu, K. Harada, J. Zhang, M. Sugiyama, M. Mizokami, and K.**
964 **Shimotohno.** 2015. Novel reporter system to monitor early stages of the hepatitis B virus
965 life cycle. Cancer Sci **106:**1616-24.
966 44. **Orzalli, M. H., and D. M. Knipe.** 2014. Cellular sensing of viral DNA and viral evasion
967 mechanisms. Annu Rev Microbiol **68:**477-92.
968 45. **Park, Y. K., E. S. Park, D. H. Kim, S. H. Ahn, S. H. Park, A. R. Lee, S. Park, H. S. Kang, J. H. Lee,**
969 **J. M. Kim, S. K. Lee, K. H. Lim, N. Isorce, S. Tong, F. Zoulim, and K. H. Kim.** 2016. Cleaved c-
970 FLIP mediates the antiviral effect of TNF-alpha against hepatitis B virus by dysregulating
971 hepatocyte nuclear factors. J Hepatol **64:**268-277.
972 46. **Qu, B., Y. Ni, F. A. Lempp, F. W. R. Vondran, and S. Urban.** 2018. T5 Exonuclease Hydrolysis
973 of Hepatitis B Virus Replicative Intermediates Allows Reliable Quantification and Fast Drug
974 Efficacy Testing of Covalently Closed Circular DNA by PCR. J Virol **92**.
975 47. **Quarleri, J.** 2014. Core promoter: a critical region where the hepatitis B virus makes
976 decisions. World J Gastroenterol **20:**425-35.
977 48. **Raney, A. K., J. L. Johnson, C. N. Palmer, and A. McLachlan.** 1997. Members of the nuclear
978 receptor superfamily regulate transcription from the hepatitis B virus nucleocapsid
979 promoter. J Virol **71:**1058-71.
980 49. **Rushmore, T. H., M. R. Morton, and C. B. Pickett.** 1991. The antioxidant responsive element.
981 Activation by oxidative stress and identification of the DNA consensus sequence required
982 for functional activity. J Biol Chem **266:**11632-9.
983 50. **Sakurai, F., S. Mitani, T. Yamamoto, K. Takayama, M. Tachibana, K. Watashi, T. Wakita, S.**
984 **Iijima, Y. Tanaka, and H. Mizuguchi.** 2017. Human induced-pluripotent stem cell-derived
985 hepatocyte-like cells as an in vitro model of human hepatitis B virus infection. Sci Rep
986 **7:**45698.
987 51. **Sandelin, A., W. Alkema, P. Engstrom, W. W. Wasserman, and B. Lenhard.** 2004. JASPAR:
988 an open-access database for eukaryotic transcription factor binding profiles. Nucleic Acids
989 Res **32:**D91-4.
990 52. **Schoggins, J. W., D. A. MacDuff, N. Imanaka, M. D. Gainey, B. Shrestha, J. L. Eitson, K. B.**
991 **Mar, R. B. Richardson, A. V. Ratushny, V. Litvak, R. Dabelic, B. Manicassamy, J. D. Aitchison,**
992 **A. Aderem, R. M. Elliott, A. Garcia-Sastre, V. Racaniello, E. J. Snijder, W. M. Yokoyama, M.**
993 **S. Diamond, H. W. Virgin, and C. M. Rice.** 2014. Pan-viral specificity of IFN-induced genes
994 reveals new roles for cGAS in innate immunity. Nature **505:**691-5.
995 53. **Schreiner, S., S. Kinkley, C. Burck, A. Mund, P. Wimmer, T. Schubert, P. Groitl, H. Will, and**
996 **T. Dobner.** 2013. SPOC1-mediated antiviral host cell response is antagonized early in human
997 adenovirus type 5 infection. PLoS Pathog **9:**e1003775.
998 54. **Shiromoto, F., H. H. Aly, H. Kudo, K. Watashi, A. Murayama, N. Watanabe, X. Zheng, T.**
999 **Kato, K. Chayama, M. Muramatsu, and T. Wakita.** 2018. IL-1beta/ATF3-mediated induction
1000 of Ski2 expression enhances hepatitis B virus x mRNA degradation. Biochem Biophys Res
1001 Commun **503:**1854-1860.
1002 55. **Sugiyama, M., Y. Tanaka, T. Kato, E. Orito, K. Ito, S. K. Acharya, R. G. Gish, A. Kramvis, T.**
1003 **Shimada, N. Izumi, M. Kaito, Y. Miyakawa, and M. Mizokami.** 2006. Influence of hepatitis
1004 B virus genotypes on the intra- and extracellular expression of viral DNA and antigens.
1005 Hepatology **44:**915-24.

1006 56. **Sun, J., A. Muto, H. Hoshino, A. Kobayashi, S. Nishimura, M. Yamamoto, N. Hayashi, E. Ito,**
1007 **and K. Igarashi.** 2001. The promoter of mouse transcription repressor bach1 is regulated by
1008 Sp1 and trans-activated by Bach1. J Biochem **130:**385-92.
1009 57. **Thomas, H., S. Senkel, S. Erdmann, T. Arndt, G. Turan, L. Klein-Hitpass, and G. U. Ryffel.**
1010 2004. Pattern of genes influenced by conditional expression of the transcription factors
1011 HNF6, HNF4alpha and HNF1beta in a pancreatic beta-cell line. Nucleic Acids Res **32:**e150.
1012 58. **Wang, H., S. Kim, and W. S. Ryu.** 2009. DDX3 DEAD-Box RNA helicase inhibits hepatitis B
1013 virus reverse transcription by incorporation into nucleocapsids. J Virol **83:**5815-24.
1014 59. **Wang, H., P. Maechler, P. A. Antinozzi, K. A. Hagenfeldt, and C. B. Wollheim.** 2000.
1015 Hepatocyte nuclear factor 4alpha regulates the expression of pancreatic beta -cell genes
1016 implicated in glucose metabolism and nutrient-induced insulin secretion. J Biol Chem
1017 **275:**35953-9.
1018 60. **Wang, Y., L. Cui, G. Yang, J. Zhan, L. Guo, Y. Chen, C. Fan, D. Liu, and D. Guo.** 2019. Hepatitis
1019 B e Antigen Inhibits NF-kappaB Activity by Interrupting K63-Linked Ubiquitination of NEMO.
1020 J Virol **93**.
1021 61. **Watashi, K., G. Liang, M. Iwamoto, H. Marusawa, N. Uchida, T. Daito, K. Kitamura, M.**
1022 **Muramatsu, H. Ohashi, T. Kiyohara, R. Suzuki, J. Li, S. Tong, Y. Tanaka, K. Murata, H. Aizaki,**
1023 **and T. Wakita.** 2013. Interleukin-1 and tumor necrosis factor-alpha trigger restriction of
1024 hepatitis B virus infection via a cytidine deaminase activation-induced cytidine deaminase
1025 (AID). J Biol Chem **288:**31715-27.
1026 62. **Wieland, S., R. Thimme, R. H. Purcell, and F. V. Chisari.** 2004. Genomic analysis of the host
1027 response to hepatitis B virus infection. Proc Natl Acad Sci U S A **101:**6669-74.
1028 63. **Wustenhagen, E., F. Boukhallouk, I. Negwer, K. Rajalingam, F. Stubenrauch, and L. Florin.**
1029 2018. The Myb-related protein MYPOP is a novel intrinsic host restriction factor of
1030 oncogenic human papillomaviruses. Oncogene **37:**6275-6284.
1031 64. **Xia, Y., D. Stadler, J. Lucifora, F. Reisinger, D. Webb, M. Hosel, T. Michler, K. Wisskirchen,**
1032 **X. Cheng, K. Zhang, W. M. Chou, J. M. Wettengel, A. Malo, F. Bohne, D. Hoffmann, F. Eyer,**
1033 **R. Thimme, C. S. Falk, W. E. Thasler, M. Heikenwalder, and U. Protzer.** 2016. Interferon-
1034 gamma and Tumor Necrosis Factor-alpha Produced by T Cells Reduce the HBV Persistence
1035 Form, cccDNA, Without Cytolysis. Gastroenterology **150:**194-205.
1036 65. **Yu, X., and J. E. Mertz.** 1997. Differential regulation of the pre-C and pregenomic promoters
1037 of human hepatitis B virus by members of the nuclear receptor superfamily. J Virol **71:**9366-
1038 74.
1039 66. **Yu, Y., P. Wan, Y. Cao, W. Zhang, J. Chen, L. Tan, Y. Wang, Z. Sun, Q. Zhang, Y. Wan, Y. Zhu,**
1040 **F. Liu, K. Wu, Y. Liu, and J. Wu.** 2017. Hepatitis B Virus e Antigen Activates the Suppressor
1041 of Cytokine Signaling 2 to Repress Interferon Action. Sci Rep **7:**1729.
1042 67. **Zhou, W., Y. Ma, J. Zhang, J. Hu, M. Zhang, Y. Wang, Y. Li, L. Wu, Y. Pan, Y. Zhang, X. Zhang,**
1043 **Z. Zhang, H. Li, L. Lu, L. Jin, J. Wang, Z. Yuan, and J. Liu.** 2017. Predictive model for
1044 inflammation grades of chronic hepatitis B: Large-scale analysis of clinical parameters and
1045 gene expressions. Liver Int **37:**1632-1641.

1046

1047

Fig. 1

A

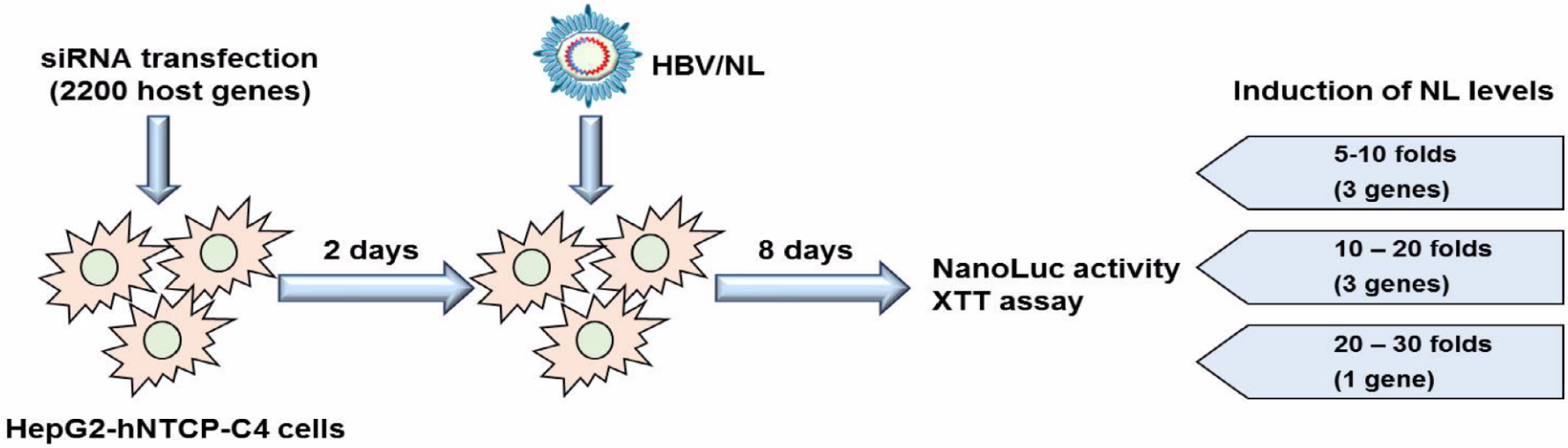
siRNA transfection
(2200 host genes)
HBV/NL
Induction of NL levels
5-10 folds
(3 genes)
2 days
8 days
NanoLuc activity
XTT assay
10 – 20 folds
(3 genes)
20 – 30 folds
(1 gene)
HepG2-hNTCP-C4 cells

B

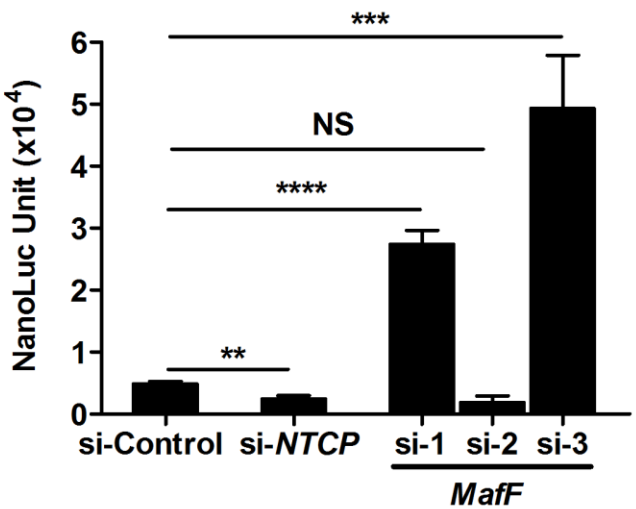
***
NS
****
**
NanoLuc Unit (x10^4)
0
1
2
3
4
5
6
si-Control
si-NTCP
si-1
si-2
si-3
MafF

C

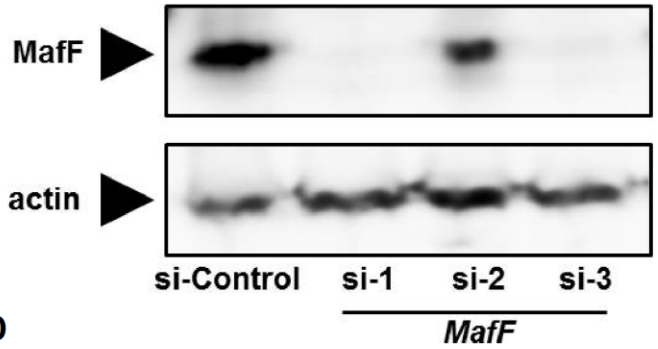
MafF
actin
si-Control
si-1
si-2
si-3
MafF

D

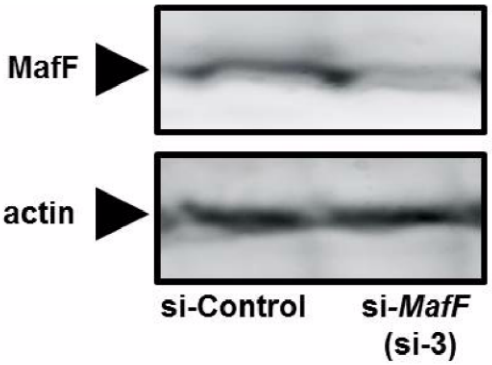
MafF
actin
si-Control
si-MafF
(si-3)

Fig. 2

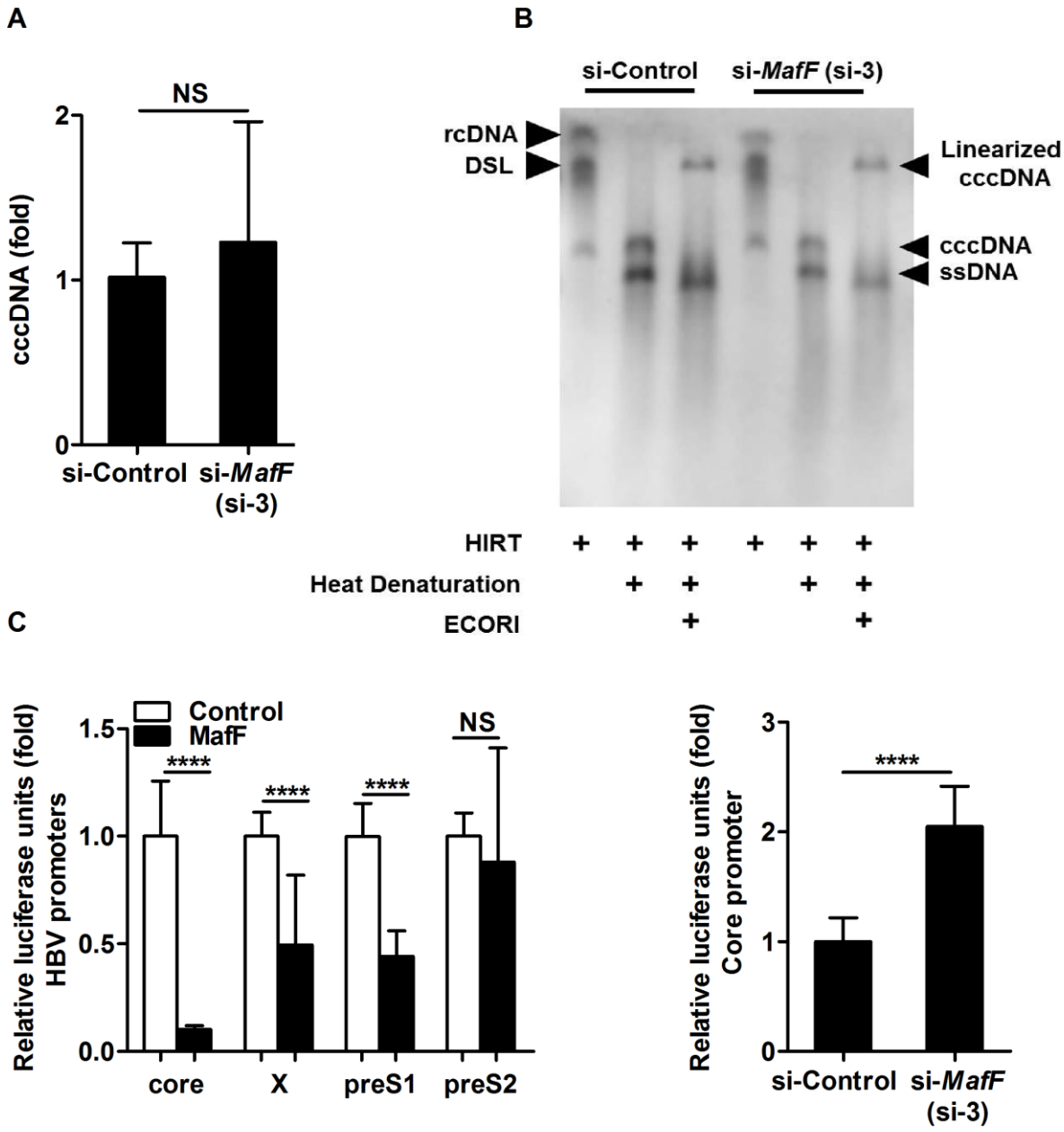
A
NS
cccDNA (fold)
2
1
0
si-Control
si-MafF (si-3)
B
si-Control
si-MafF (si-3)
rcDNA
DSL
Linearized cccDNA
cccDNA
ssDNA
HIRT
Heat Denaturation
ECORI
C
Control
MafF
Relative luciferase units (fold)
HBV promoters
1.5
1.0
0.5
0.0
****
****
****
NS
core
X
preS1
preS2
Relative luciferase units (fold)
Core promoter
3
2
1
0
****
si-Control
si-MafF (si-3)

Fig. 3

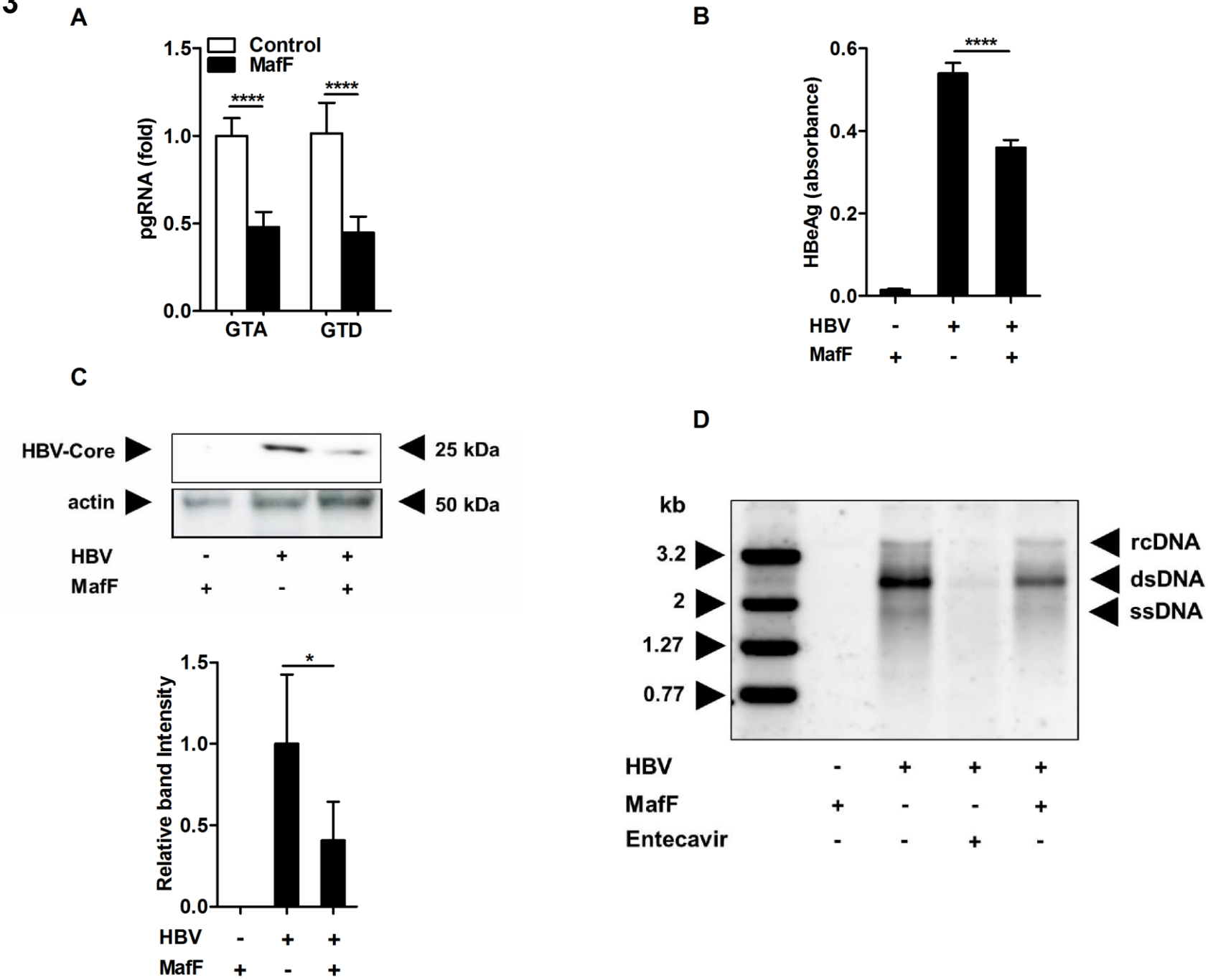
A
Control
MafF
pgRNA (fold)
1.5
1.0
0.5
0.0
****
****
GTA
GTD
B
HBeAg (absorbance)
0.6
0.4
0.2
0.0
****
HBV - + +
MafF + - +
C
HBV-Core
actin
25 kDa
50 kDa
HBV - + +
MafF + - +
Relative band Intensity
1.5
1.0
0.5
0.0
*
HBV - + +
MafF + - +
D
kb
3.2
2
1.27
0.77
rcDNA
dsDNA
ssDNA
HBV - + + +
MafF + - - +
Entecavir - - + -

Fig. 4

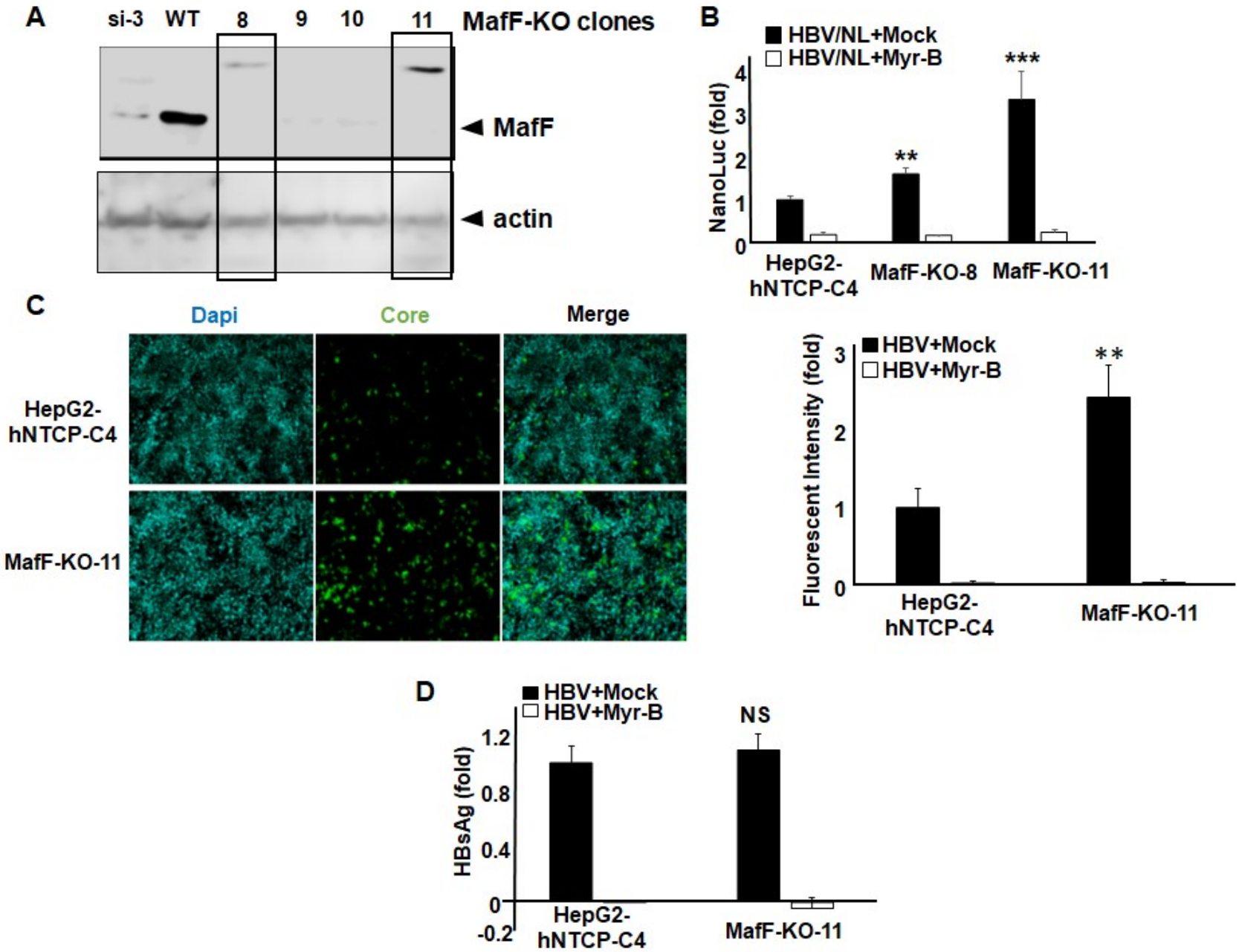
A
si-3
WT
8
9
10
11
MafF-KO clones
MafF
actin
B
HBV/NL+Mock
HBV/NL+Myr-B
NanoLuc (fold)
0
1
2
3
4
**
***
HepG2-hNTCP-C4
MafF-KO-8
MafF-KO-11
C
Dapi
Core
Merge
HepG2-hNTCP-C4
MafF-KO-11
HBV+Mock
HBV+Myr-B
Fluorescent Intensity (fold)
0
1
2
3
**
HepG2-hNTCP-C4
MafF-KO-11
D
HBV+Mock
HBV+Myr-B
HBsAg (fold)
1.2
0.8
0.4
0
-0.2
NS
HepG2-hNTCP-C4
MafF-KO-11

Fig. 5

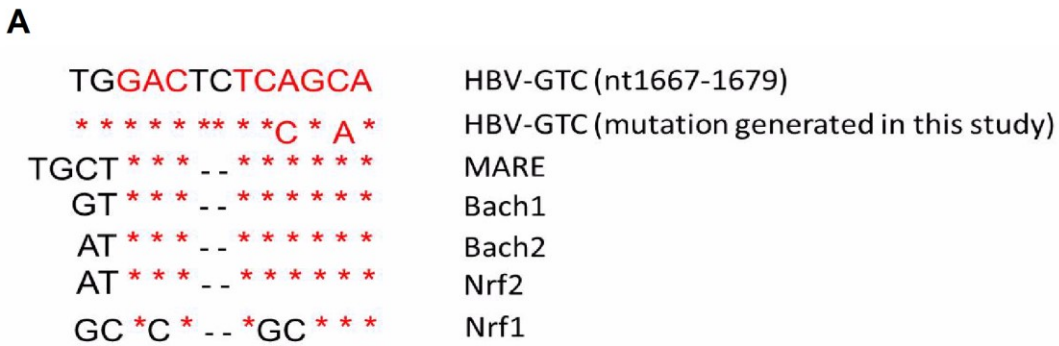
A
TGGACTCTCAGCA
HBV-GTC (nt1667-1679)
* * * * * ** * *C * A *
HBV-GTC (mutation generated in this study)
TGCT * * * - - * * * * * *
MARE
GT * * * - - * * * * * *
Bach1
AT * * * - - * * * * * *
Bach2
AT * * * - - * * * * * *
Nrf2
GC *C * - - *GC * * *
Nrf1

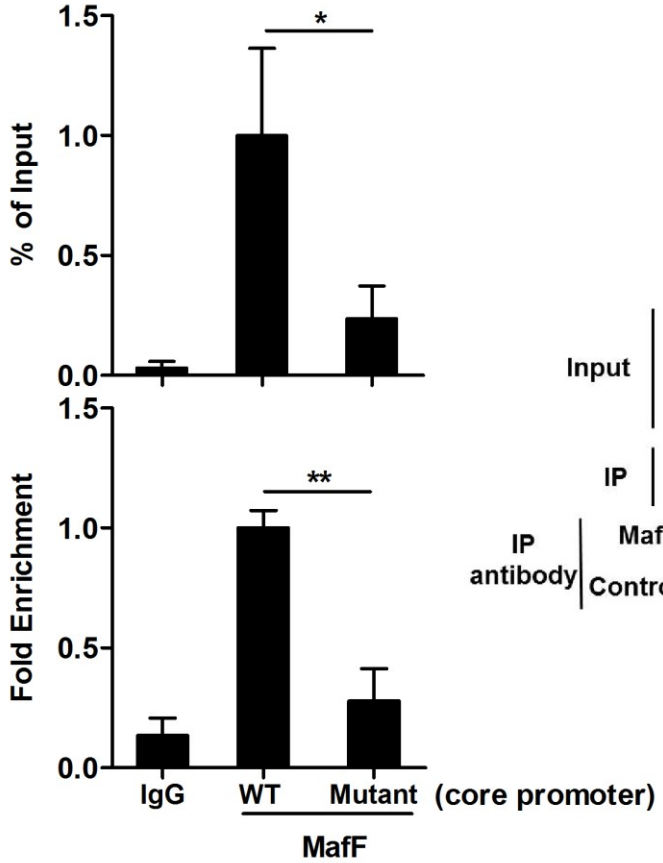
C
% of Input
1.5
1.0
0.5
0.0
*
Fold Enrichment
**
IgG
WT
Mutant
(core promoter)
MafF

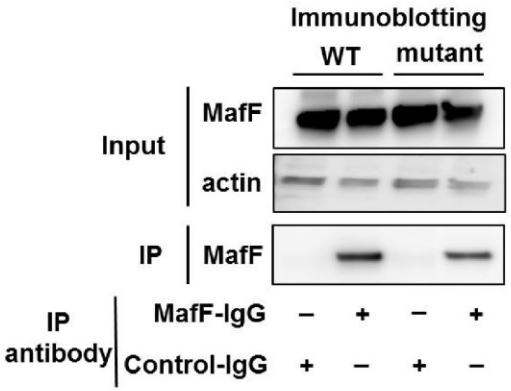
Immunoblotting
WT
mutant
Input
MafF
actin
IP
MafF
IP antibody
MafF-IgG
Control-IgG

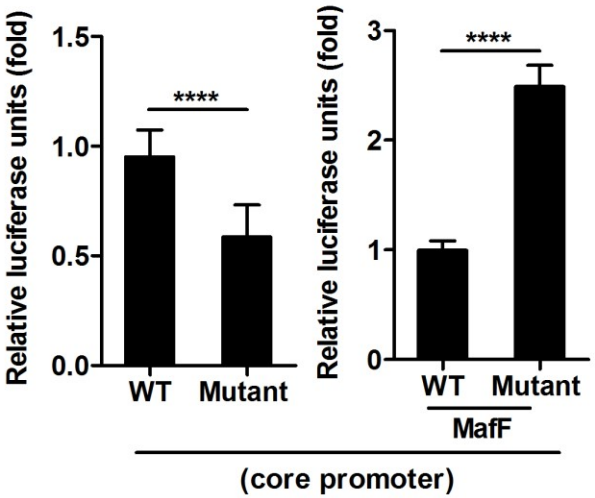
B
Relative luciferase units (fold)
1.5
1.0
0.5
0.0
****
WT
Mutant
3
2
1
0
MafF
(core promoter)

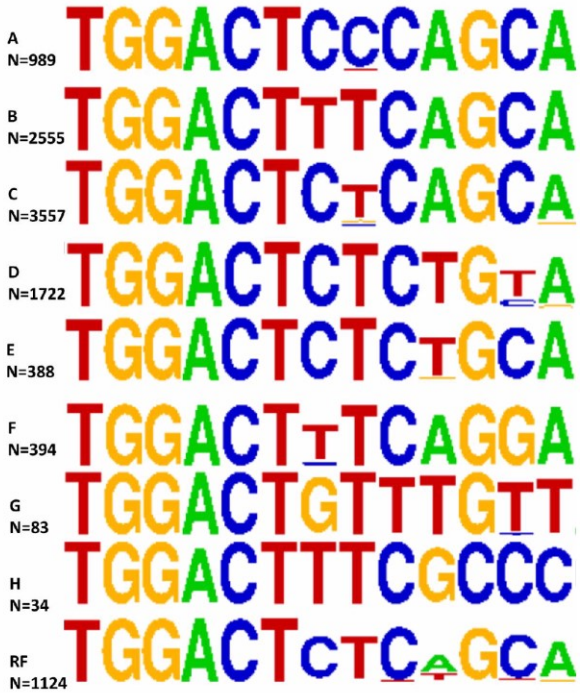
D
A N=989
B N=2555
C N=3557
D N=1722
E N=388
F N=394
G N=83
H N=34
RF N=1124

Fig. 6

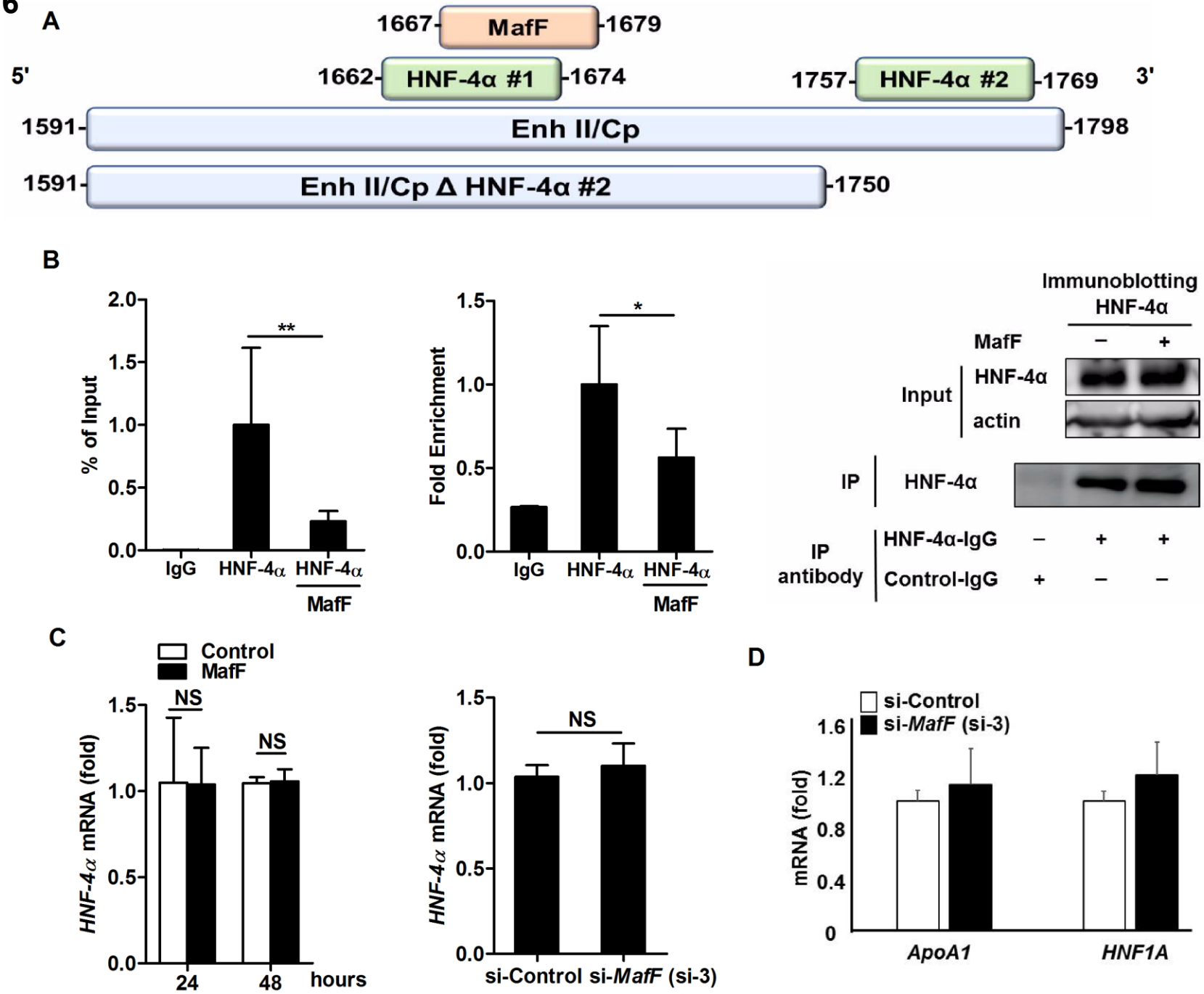
A
1667-
MafF
-1679
5'
1662-
HNF-4α #1
-1674
1757-
HNF-4α #2
-1769
3'
1591-
Enh II/Cp
-1798
1591-
Enh II/Cp Δ HNF-4α #2
-1750
B
% of Input
2.0
1.5
1.0
0.5
0.0
**
IgG
HNF-4α
HNF-4α
MafF
Fold Enrichment
1.5
1.0
0.5
0.0
*
IgG
HNF-4α
HNF-4α
MafF
Immunoblotting
HNF-4α
MafF
–
+
Input
HNF-4α
actin
IP
HNF-4α
IP antibody
HNF-4α-IgG
–
+
+
Control-IgG
+
–
–
C
Control
MafF
HNF-4α mRNA (fold)
1.5
1.0
0.5
0.0
NS
NS
24
48
hours
HNF-4α mRNA (fold)
1.5
1.0
0.5
0.0
NS
si-Control
si-MafF (si-3)
D
si-Control
si-MafF (si-3)
mRNA (fold)
1.6
1.2
0.8
0.4
0
ApoA1
HNF1A

Fig. 7

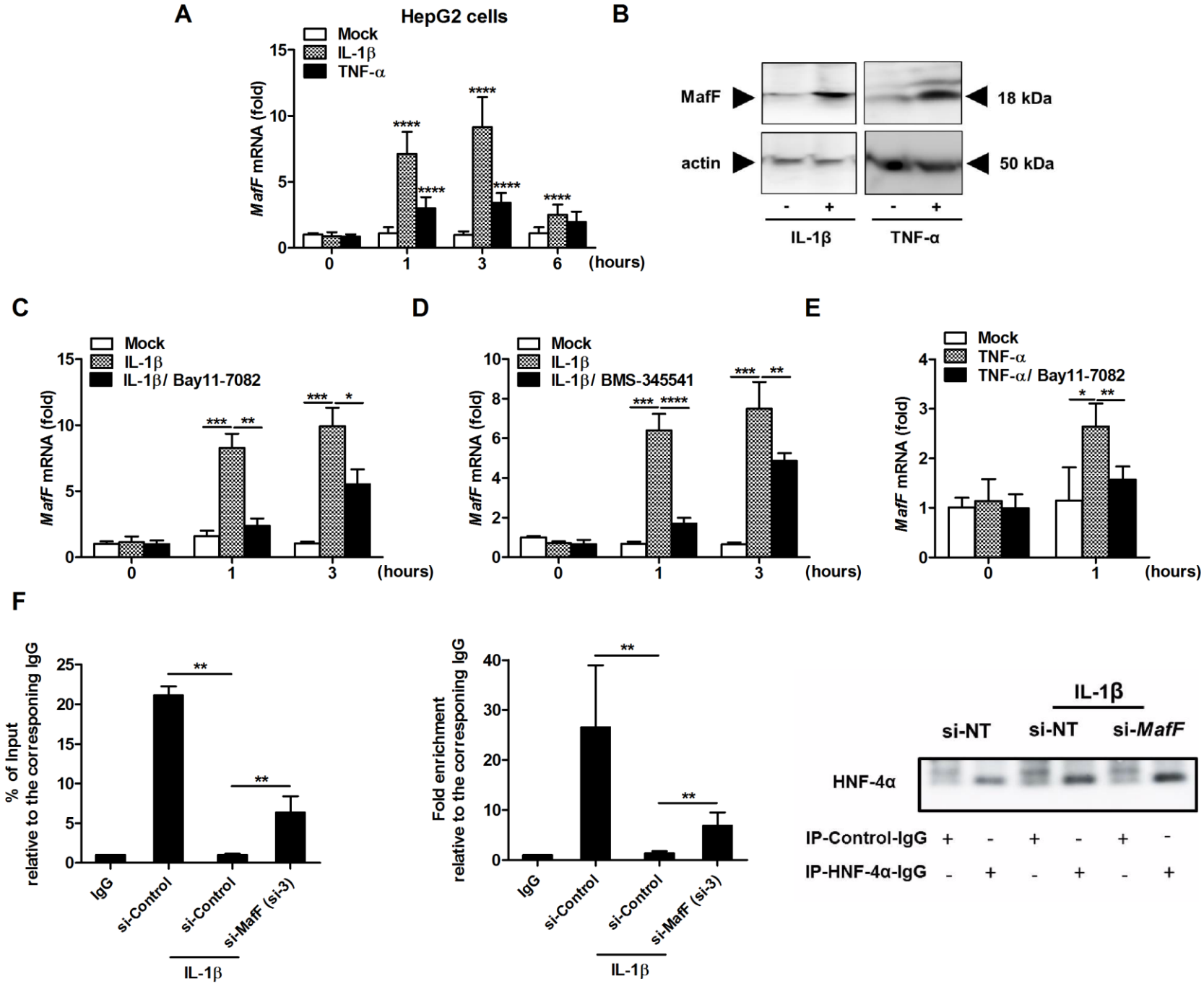
A
HepG2 cells
Mock
IL-1β
TNF-α
MafF mRNA (fold)
(hours)
B
MafF
actin
18 kDa
50 kDa
IL-1β
TNF-α
C
IL-1β/ Bay11-7082
D
IL-1β/ BMS-345541
E
TNF-α/ Bay11-7082
F
% of Input relative to the corresponing IgG
Fold enrichment relative to the corresponing IgG
IgG
si-Control
si-MafF (si-3)
si-NT
si-MafF
HNF-4α
IP-Control-IgG
IP-HNF-4α-IgG

Fig. 8

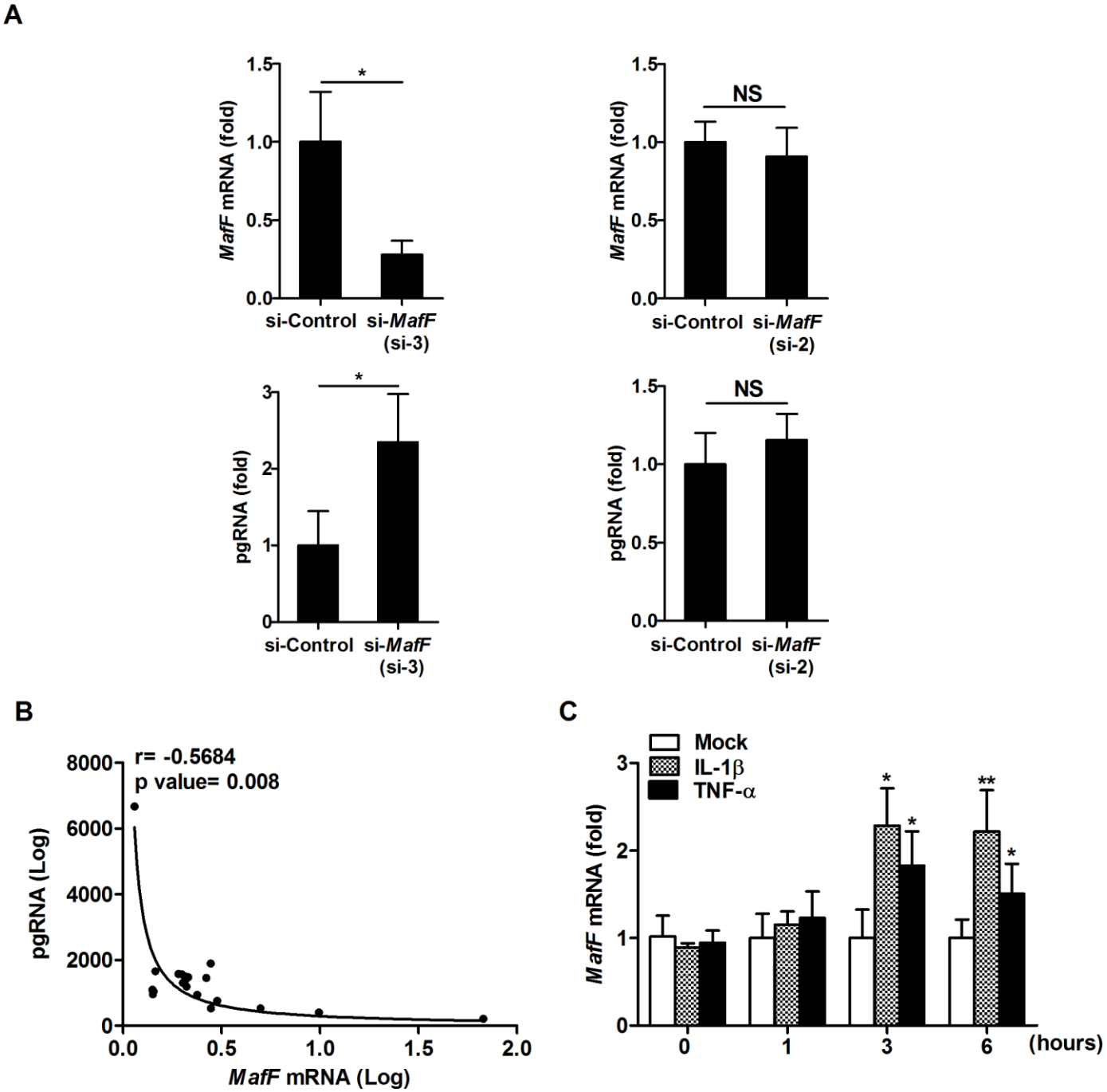
A
MafF mRNA (fold)
1.5
1.0
0.5
0.0
*
si-Control
si-MafF (si-3)
NS
si-MafF (si-2)
pgRNA (fold)
3
2
1
0
B
r= -0.5684
p value= 0.008
8000
6000
4000
2000
0
pgRNA (Log)
0.0
0.5
1.0
1.5
2.0
MafF mRNA (Log)
C
Mock
IL-1β
TNF-α
**
0
1
3
6
(hours)

Fig. 9

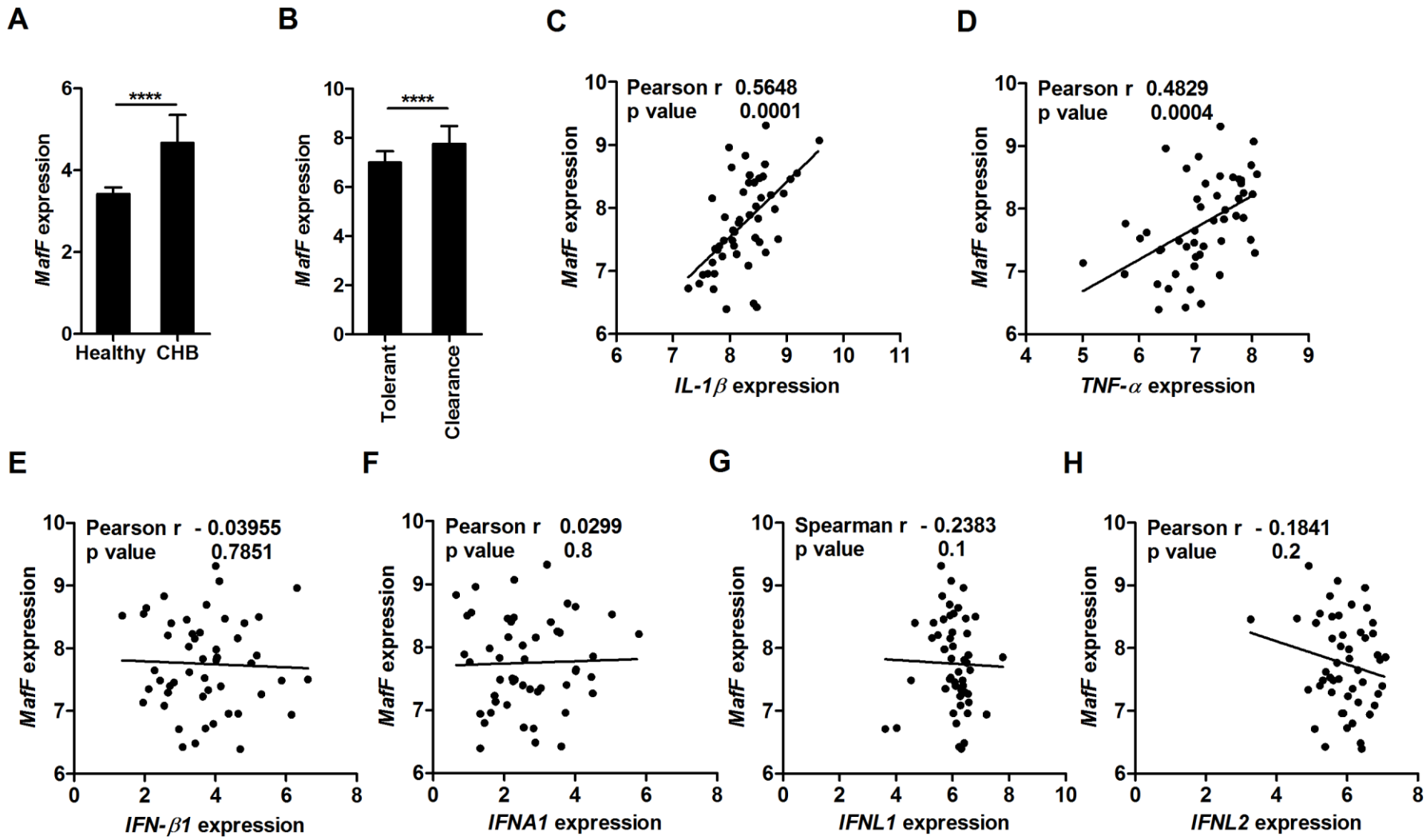
A
MafF expression
****
Healthy
CHB
B
MafF expression
****
Tolerant
Clearance
C
Pearson r 0.5648
p value 0.0001
MafF expression
IL-1β expression
D
Pearson r 0.4829
p value 0.0004
MafF expression
TNF-α expression
E
Pearson r - 0.03955
p value 0.7851
MafF expression
IFN-β1 expression
F
Pearson r 0.0299
p value 0.8
MafF expression
IFNA1 expression
G
Spearman r - 0.2383
p value 0.1
MafF expression
IFNL1 expression
H
Pearson r - 0.1841
p value 0.2
MafF expression
IFNL2 expression